Extrapolation of Mean Wind Statistics with Special Regard to Wind Energy Applications. WMO. World Climate Programme Report No. WCP-86

Jensen, Niels Otto; Lundtang Petersen, Erik; Troen, I.

Publication date:
1984

Document Version
Publisher's PDF, also known as Version of record

WORLD CLIMATE PROGRAMME

DATA • APPLICATION • IMPACT • RESEARCH

WORLD CLIMATE APPLICATIONS PROGRAMME

EXTRAPOLATION OF MEAN WIND STATISTICS WITH SPECIAL REGARD TO WIND ENERGY APPLICATIONS

by

Niels Otto Jensen, Erik Lundtang Petersen and Ib Troen
Risø National Laboratory, Denmark

WCP - 86

WORLD METEOROLOGICAL ORGANIZATION

(August 1984)

WMO/TD-No. 15

FOREWORD

The development of wind energy calls for the contribution of meteorologists during all phases of implementation of wind energy systems, from the very first general wind energy resource assessment of a region to the management of windmills or aero-generators once they are built. This is the basic reason why, for many years, the World Meteorological Organization has been involved in various wind energy related activities and, among others, in an active publication programme which has resulted in two important volumes on this topic:

The WMO Technical Note no. 175 "Meteorological Aspects of the Utilization of Wind Energy as an Energy Source", published in 1981, reviewed the whole of the question and was addressed to both the meteorologist and the wind energy technologist with the basic aim of introducing each to the other: the latter should know what assistance can be provided by the meteorologists and how, and the former should be aware of the questions he will have to answer and why.

In 1983, another publication of WMO was devoted to wind energy: the second part of "Climate Applications Referral System (CARS)/Solar energy, Wind energy" (WCP no. 56) provides information on concrete, practical methods of meteorology as applied to wind energy questions. Following a simple description of each method, references are given indicating where more information can be sought, if needed.

The objective of the present publication "Extrapolation of mean wind statistics with special regard to wind energy applications" is to review present knowledge about one of the most important questions related to wind energy development in an area. "What can be said about the behaviour of wind in places where no measurements are made?". The different aspects of this question - vertical extrapolation, horizontal extrapolation, assessment of the influence of underlying surface roughness, estimation of the perturbations induced by terrain features - are considered here with the pragmatic view of the specialist in applied climatology but without over-simplification.

This difficult task of achieving an acceptable compromise between the useful and the true was carried out by Drs. N.O. Jensen, E.L. Petersen and I. Troen of the Risø National Laboratory (Røskilde, Denmark). I thank them for this important contribution to the World Climate Programme.

(G.O.P. Obasi)
Secretary-General

CONTENTS

ABSTRACT

To help wind energy decision-makers, meteorologists must know how to extrapolate wind data because data often do not exist for the site where the wind machine is to be located. This report is devoted to both the vertical and the horizontal extrapolations of the mean wind speed. Basic notions and explanations on "wind energy meteorology" can be found in WMO Technical Note 175 "Meteorological Aspects of the Utilization of Wind as an Energy Source".

The report introduces in Chapter 2 the notion of "mean" wind speed as seen from the point of view of the wind energy engineer. Chapter 3 describes the power curve of a wind machine and shows why the use of a Weibull distribution for fitting wind speed data (when it is possible) is particularly convenient for further analysis of energy production. An analysis of the Weibull distribution is provided to the reader in Chapter 4, with examples related to wind study.

Chapter 5 is devoted to the vertical profile of wind under "ideal" conditions, i.e. when the underlying surface is horizontal and homogeneous. The influences of the atmospheric stability and of the underlying surface roughness are analysed both from a theoretical and from an empirical point of view, leading to the presentation of practical methods for vertical extrapolation. The perturbations caused by simple changes in underlying surface conditions are given in Chapter 6, which suggests practical ways to tackle with this problem. Chapter 7 focuses on the perturbations induced by "low terrain features" that is to say by smooth topographic variability; theoretical elements are provided as well as empirical methods to estimate the effects of ridges and escarpments. Some corrections that can be introduced to correct for local shelter effects (e.g. buildings) are listed in Chapter 8.

Horizontal extrapolation is covered in Chapter 9 stressing the fact that, in practice, horizontal and vertical extrapolations are linked problems: the authors suggest not to try to directly interpolate mean wind speed between stations (even after careful screening or corrections) but rather to go through the intermediary of the geostrophic wind. Related example of national and international studies are provided. Chapter 10 describes on-going research about wind flows in complicated terrains (e.g. mountains) where many different mechanical and thermal effects should be analysed. Chapter 11 considers some questions related to wind data measurement, and handling. Finally, Chapter 12 provides the reader with a wide bibliography related to the whole subject of the report.

1. INTRODUCTION

The renewed interest in the use of wind energy has led to a number of investigations addressing the problem of assessing the wind climate of a region or a specific location. In general the available observational data refer neither to the height nor the locations of interest for siting of wind turbines. Therefore it is almost always necessary to perform vertical and horizontal extrapolation of the data. This report deals with the theory for horizontal and vertical extrapolation of mean wind speed. The main discussion focuses on the wind structure over simple complex terrain. With the term simple complex terrain is meant terrain which conform to types which are dealt with in contemporary literature, e.g. step changes in surface roughness or temperature, or moderate changes in surface elevation. However, Chapter 10 offers some comments on winds in real, complicated terrain.

With respect to the concrete use of meteorological information in the field of wind energy reference is made to the Climate Applications Referral System, Wind Energy (WCP-56, WMO 1983). The referral system provides references including review of proven methods tried, tested and operationally used in some region or country.

2. DEFINITION OF MEAN WIND SPEED

Due to the finite response time of the rotor system on a wind generator, it is not necessary to attempt very short time averaging or rapid sampling of wind statistics for turbine output calculation. The relative error, Δ, in the estimate by fast sampled winds can be shown to be of order

$$\Delta \simeq 3\left(\frac{\sigma}{\bar{u}}\right)^2 \qquad (2.1)$$

where σ is the standard deviation of the wind speed u relative to the average value $\bar{u}$ sensed by the turbine. Here overbar indicates a time averaged value. The question now is what is the appropriate averaging time?

Irrespective of how fast parts of the rotor system react to changes in wind speed (i.e. how rapid circulation build up on a local blade segment) the total time response may be limited by the spatial extend of the entire rotor. This is due to the lack of lateral and vertical coherence in the wind field. The coherence may be expressed as (Kristensen and Jensen, 1979)

$$\text{coh} = \exp\left(-a\,\frac{nD}{\bar{u}}\right) \qquad (2.2)$$

where n is the turbulent eddy frequency which is being considered, and D is the spatial displacement between two points in which the wind is being observed (i.e. in this case the rotor diameter). At heights relevant for wind generators, the constant a is of order 10 (Kristensen et al., 1981).

Thus for a reasonable (0.6) coherence over the rotor area the argument in the exponent in eq. (2.2) should be less than or equal to 0.5, or equivalently

$$n < 0.5\,\frac{\bar{u}}{nD} \qquad (2.3)$$

which means that all frequencies larger than the right-hand side value are being filtered out to a larger or smaller degree. In terms of averaging time this means that the only relevant values of T are

$$T > 2\,aD/\bar{u} \qquad (2.4)$$

which for usual values of the involved parameters amount to the order of 1 min.

Thus the averaging time of σ and $\bar{u}$ in Eq. (2.1) are akin to normal micrometeorological usage in which $\sigma/\bar{u}$ is typically 0.2, which amounts to an overestimation of $\Delta \simeq 10\%$ if instantaneous wind values are used rather than proper averages. However, mostly this is not the problem.

On the other hand, much larger averaging times will cause the energy production to be estimated too low. If for example one would use the daily average speed, and the local wind climate consisted of a breeze situation in which a generator could only be on or off, and for simplicity the split between these two states were 50%, the ratio between the energy production using the average wind speed only and the true energy production would be

$$(\tfrac{1}{2} u_m)^3 / \tfrac{1}{2} u_m^3 = 1/4 \qquad (2.5)$$

where u_m is the maximum wind speed during the day. Thus in this case the energy estimate is in error (too low) with a factor of four. Thus the averaging time should be chosen as low as possible, but not necessarily lower than of the order of a few minutes. Use of standard 10 min. average data seems adequate.

This is in agreement with the IEA-recommended averaging time for "power curve" determination (Frandsen et al., 1982) which is based on the requirements for getting good statistical dependency between simultaneous measurements of wind speed and generator output (Frandsen and Christensen, 1980). It also agrees with the WMO/CAS (1971) recommendation on observational requirements. The discussion in the chapters to follow implicitly assume that data are 10 min. averages values. The last chapter discusses the use of other data.

3. ESTIMATION OF WIND POWER

3.1. Power density

The energy flux (power density) in a flow of air through a unit area at right angles to the surface of the earth is given by

$$E(u) = \frac{1}{2} \text{ (mass per second per } m^2) \text{ (speed)}^2$$

$$= \frac{1}{2} \rho u^3 \ (kgs^{-3}) = \frac{1}{2} \rho u^3 \ (Wm^{-2}) \qquad (3.1)$$

where

$E(u)$ = power density at wind speed u (Wm^{-2})
ρ = density of air (1.2 kgm^{-3})
u = horizontal wind speed (ms^{-1})

In Eq. (3.1) u is the instantaneous horizontal wind speed at a given point. In practical applications the wind speed will always be a measured quantity which is created from u by averaging over a time interval, as discussed in the previous chapter.

3.2. Power curve

The power curve P(u) of a wind turbine gives the energy it can produce at a given wind speed. If the turbine could make use of all the energy in the wind, the power curve of the turbine would be identical to Eq. (3.1). In practice a wind turbine will only be able to use 20-30% of the available energy. A typical power curve is shown in Fig. 3.3.

3.3. The probability density function

The mean energy production, P, for a wind turbine with power curve P(u) can be determined by

$$P = Pr_1 P(u_1) + Pr_2 P(u_2) + \ldots \qquad (3.2)$$

where the Pr's are weights that reflect the frequency of occurrence of the wind speed in a given interval. Pr_1, for example, could be the fraction of time the wind speed is in the interval from 0 to 1 ms^{-1}, and $P(u_1)$ would be taken as the value of the power characteristic at the mid-point of this interval. Figure (3.1) illustrates the weighting function Pr; this function is usually called the histogram. The sum of Pr's is exactly 1 (or 100%).

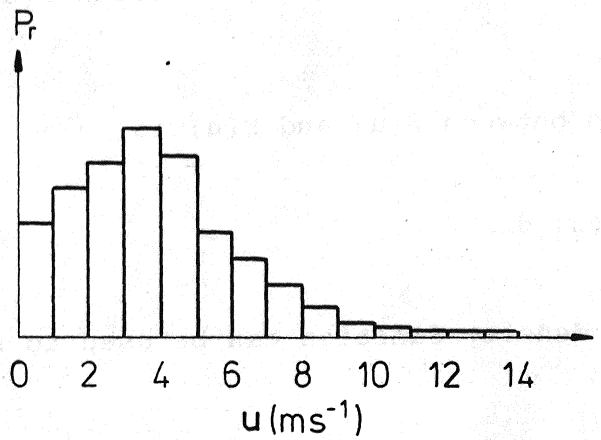

Fig. 3.1. Weighting function Pr. Histogram of wind speeds.

The probability density function is the continuous counterpart to the histogram. This function is sketched in Fig. (3.2). The shaded area gives the probability that the wind speed lies in the interval of u to u + Δu.

Figure (3.2) also shows the accumulated probability density function F(u) which gives the probability of wind speeds less than u. The probability that the wind speed is larger than u is given by 1-F(u).

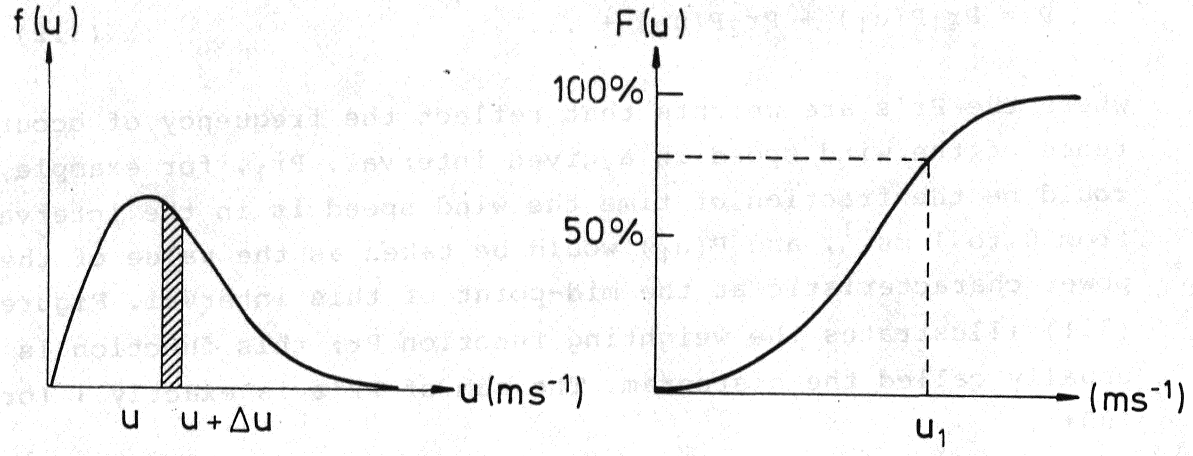

Fig. 3.2. Probability density function f(u) and accumulated probability density function F(u).

The relationship between f(u) and F(u) is

$$F(u) = \int_0^u f(u)\, du \tag{3.3}$$

The probability density function can be used to rewrite Eq. (3.2) as

$$\overline{P} = \int_0^\infty f(u)P(u)du \tag{3.4}$$

Equation (3.4) shows clearly why it is so essential for wind energy purposes to determine the probability density function of the wind speed. Not only can the mean energy production $\overline{P}$ be obtained, but also the form of the power curve P(u) can be adapted to the form of f(u), so that $\overline{P}$ becomes as large as possible, thus maximizing the output of the wind turbine.

The first, second, and third moment of the wind speed can be directly calculated from the wind speed probability density function by the following

$$\overline{u^n} = \int_0^\infty u^n f(u)du \ , \ n = 1,2,3,... \tag{3.5}$$

It follows that the mean energy density is given by

$$\overline{E} = \frac{1}{2} \rho \int_0^\infty u^3 f(u) du \qquad (3.6)$$

The probability density function f(u) can be obtained from measurements of the wind speed over an appropriate time span and with a suitable averaging time. As previously discussed the averaging time should be of the order of 10 minutes. The length of the measurement series depends upon the form of the power curve since this curve typically eliminates the influence of small wind speeds and damps the importance of the large wind speeds. This means that for wind energy purposes, shorter measurement series than are normally required for general wind climatological investigations can be used.

Usually there will not exist measurement series of wind speeds at the location where one wishes to place a wind turbine, and most certainly not at the relevant height over the terrain - the hub height. As will be described in Chapter 9 the determination of the probability density function f(u) at a given location and height will often have to rely on the fact that the measured wind speeds almost always follow a Weibull distribution. This distribution is described in detail in the following chapter.

However, for the use in the rest of this chapter we note from Chapter 4 that the Weibull distribution has two parameters A (close to the mean value) and k (determining the shape, see Fig. 4.1). The mathematical expression is given by Eq. (4.1) and the mean energy density by Eq. (4.4).

3.4. Determination of mean power production

For many wind turbines the power curve is reasonably well approximated by the simple shape shown in Fig. 3.3.

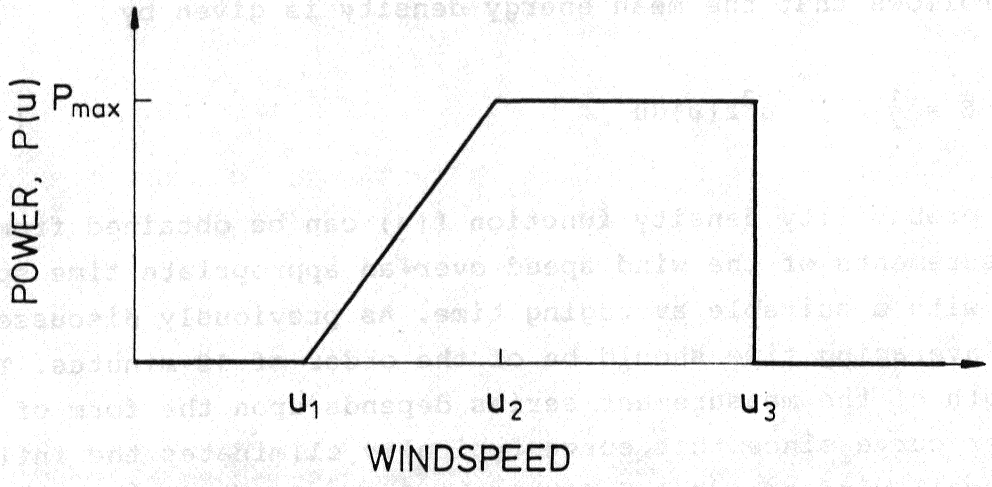

Fig. 3.3. Simple linear power curve.

When the wind speed is less than u_1, the turbine will not be able to produce power (u_1 can be referred to as the starting speed). Between u_1 and u_2 the power output increases linearly with wind speed to the value P_{max} (rated power) at wind speed u_2; thereafter the output is constant until a (possible) maximum wind speed u_3 above which the turbine must be stopped for reasons of safety. The expression for the mean power becomes in this case (Petersen et. al, 1981):

$$P = \frac{P_{max}}{\alpha_2 - \alpha_1} \{G_k(\alpha_2) - G_k(\alpha_1) - \exp(-\alpha_3^k)\} \qquad (3.7)$$

where

$$\alpha_1 = \frac{u_1}{A} \; ; \; \alpha_2 = \frac{u_2}{A} \; , \; \alpha_3 = \frac{u_3}{A} \qquad (3.8)$$

The function $G_k(\alpha)$ is 1/k times the incomplete gamma function of two arguments 1/k and αk. The function is shown in Fig. 3.4 for a range of k. In practice the last term can often be neglected since the very high wind speeds at which the turbine must be stopped occur very infrequently. Figure 3.4 provides a fast mean for calculating the production of a specific turbine for various choices of A and k. Hence an uncertainty interval

for A and k can be transformed into an uncertainty interval for the power production.

Example 3.1

A small wind turbine is to be placed at a certain site. The power curve for the turbine is measured to correspond to the simple linear shape with the parameters

starting speed $u_1 = 5\ ms^{-1}$
stalling speed $u_2 = 12\ ms^{-1}$
rated power $P_{max} = 50\ kW$

The Weibull parameters at hub height are estimated as:

$A = 6\ ms^{-1}$
$k = 2$

which gives

$\alpha_1 = 0.83$ $\quad G_k(\alpha_1) = 0.68$
$\alpha_2 = 2.00$ $\quad G_k(\alpha_2) = 0.88$
$\alpha_2 - \alpha_1 = 1.17$

from which the mean power can be calculated as:

$$P = 50\ kW \cdot \frac{1}{1.17}\ (0.88 - 0.68) = 8.5\ kW \qquad (3.9)$$

Repeating the calculations for $A = 6 \pm 1\ ms^{-1}$ and $k = 1.5$ and 3 gives:

A \ k	1.5	2	3	
5	6.8	5.0	2.9	P
6	10.7	8.5	7.3	kW
7	14.0	13.0	10.0	

If the turbine is not decided upon or the power curve not available the uncertainty calculations for variations in the Weibull parameters have to be performed on the cubic power curve

$$P \sim u^3$$

which gives (Eq. 4.4):

$$\overline{E} = \frac{1}{2} \rho A^3 \Gamma \left(1 + \frac{3}{k}\right) Wm^{-2} \qquad (3.10)$$

Using the same parameters as above and $\rho = 1.23$ kgm^{-3} gives:

A \ K	1.5	2	3	
5	152	101	76	E
6	264	175	132	Wm^{-2}
7	418	278	209	

Comparing the two tables shows large differences when A is kept constant and k is varied. However, it is seen that for k equal 2 and A varied the two methods give the same relative variation, an uncertainty interval of approximately 100%. This is due to the fact that the power curve for the wind turbine considered is close to be the optimum linear power curve with respect to a wind distribution with A = 6 ms^{-1}; k = 2 (see Petersen et al., 1981, Chapter 5).

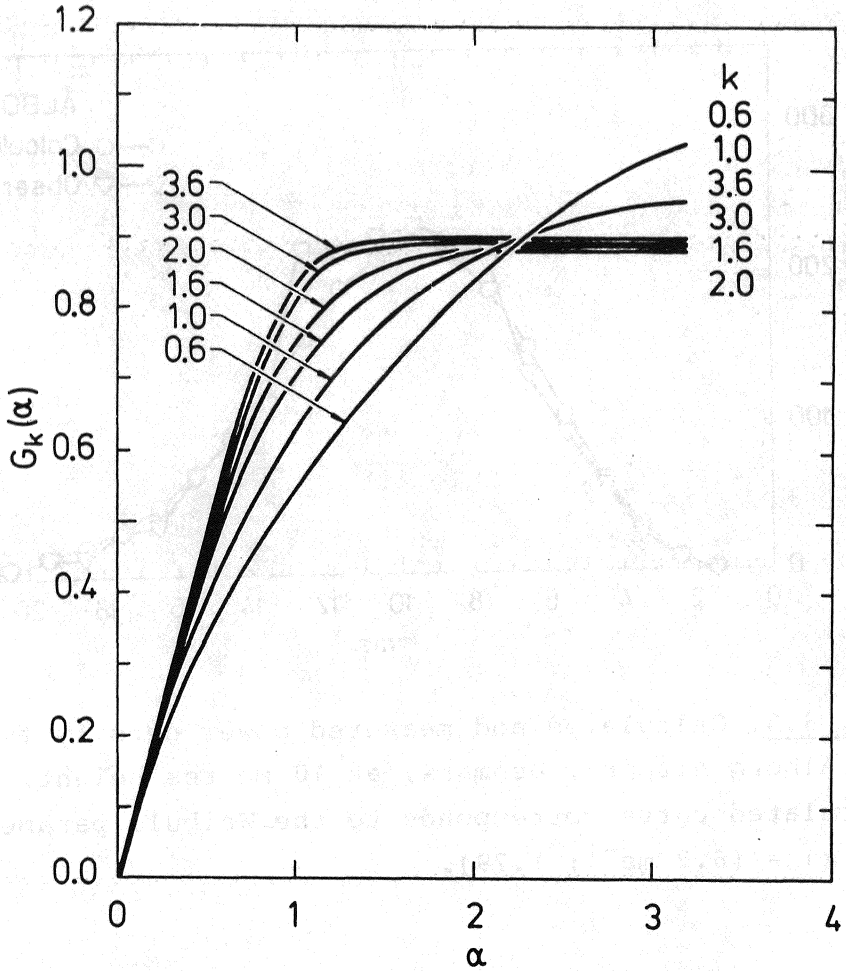

Fig. 3.4. Curves for the calculation of the mean power by means of Eq. (3.7).

3.5. Power density function

It is sometimes of interest to evaluate how different ranges of wind speeds will contribute to the power production. A very simple estimate can be made by evaluating the mean energy content in the wind for different wind speeds. The mean power density is given as

$$E(u) = \frac{1}{2} \rho u^3 \cdot f(u) \qquad (3.11)$$

where f(u) is the Weibull distribution corresponding to the situation considered. A graph of this function gives a picture of which wind speeds are important for the mean power production. An example is shown in Fig. 3.5.

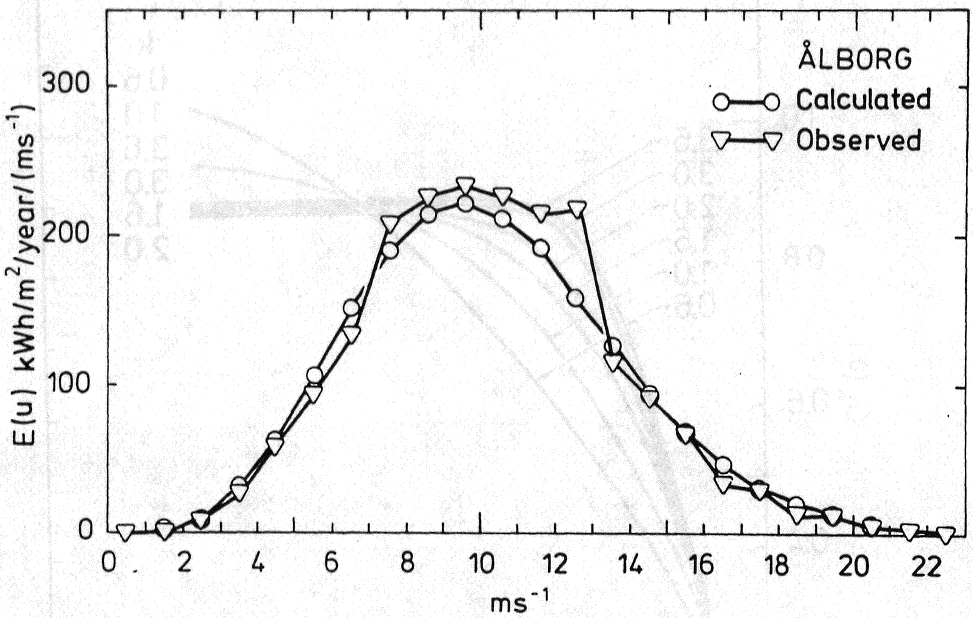

Fig. 3.5. Calculated and measured power density functions for Ålborg Airport, Denmark, at 10 metres height. The calculated curve corresponds to the Weibull parameters (A; k) = (6.2 ms^{-1}; 1.79).

3.6. Power duration curve

From the Weibull parameters and the power curve the probability that the power will exceed a certain value can be calculated. The corresponding curve is called the power duration curve.

The probability that the power will exceed P between zero and P_{max} is given by

$$Pr(\text{Power} > P) = \exp\left(-\left(\frac{u_p}{A}\right)^k\right) \qquad (3.12)$$

with

$$P = \frac{P_{max}}{u_2-u_1}(u_p-u_1) \quad \text{or} \quad u_p = u_1 + \frac{P}{P_{max}}(u_2-u_1) \qquad (3.13)$$

then

$$\Pr(\text{Power} > P) = \exp\left(-\left(\alpha_1 + \frac{P}{P_{max}}\,(\alpha_2-\alpha_1)^k\right)\right) \qquad (3.14)$$

An example is shown in Fig. 3.6.

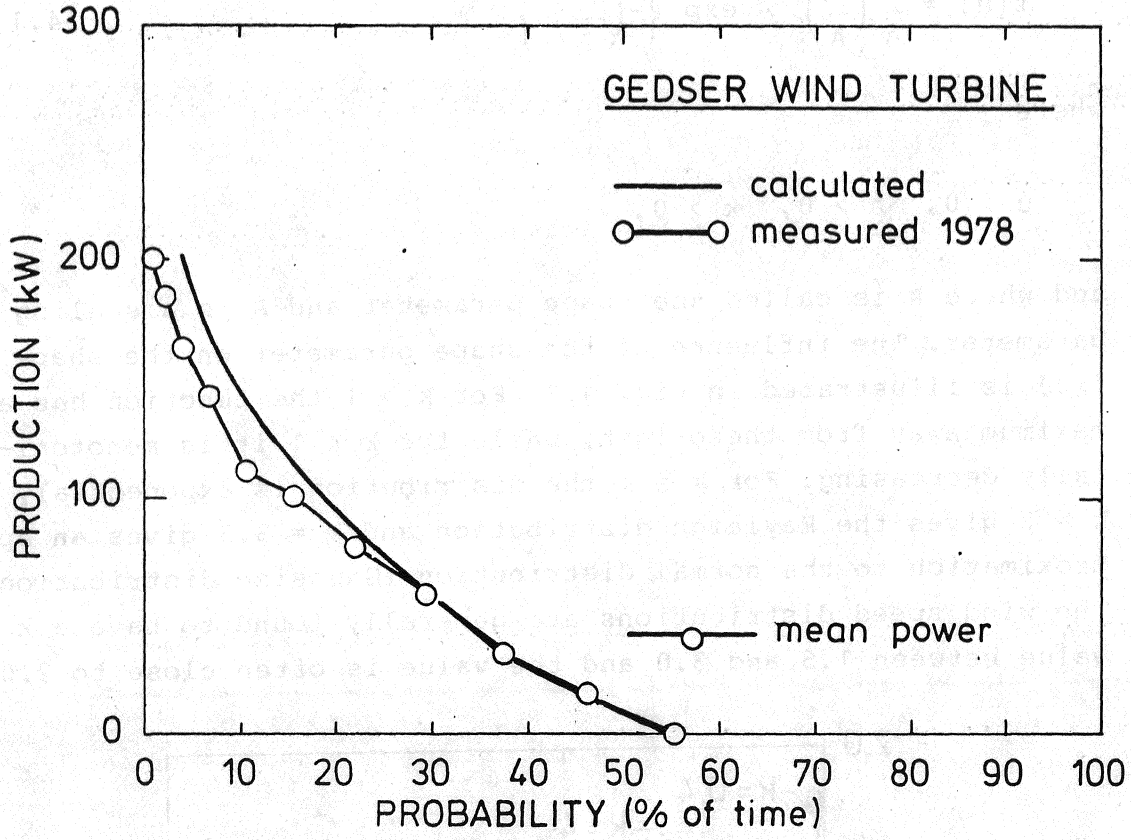

Fig. 3.6. Calculated and measured power duration curves for the Gedser wind turbine (Denmark). The calculated curve corresponds to the Weibull parameters (A; k) = (7.6 ms^{-1}; 1.76).

4. WEIBULL FREQUENCY DISTRIBUTIONS

4.1. The Weibull distribution

The Weibull distribution is expressed mathematically as

$$f(u) = \frac{k}{A}\left(\frac{u}{A}\right)^{k-1} \exp\left\{-\left(\frac{u}{A}\right)^{k}\right\} \qquad (4.1)$$

where

$$u > 0, \quad A > 0, \quad k > 0,$$

and where k is called the shape parameter and A is a scaling parameter. The influence of the shape parameter on the shape of f(u) is illustrated in Fig. 4.1. For $k > 1$ the function has a maximum away from the origin, while for $k < 1$ it is monotonically decreasing. For $k = 1$ the distribution is exponential, $k = 2$ gives the Rayleigh distribution and $k = 3.5$ gives an approximation to the normal distribution (Gaussian distribution). The wind speed distributions are generally found to have a k value between 1.5 and 3.0 and the value is often close to 2.0.

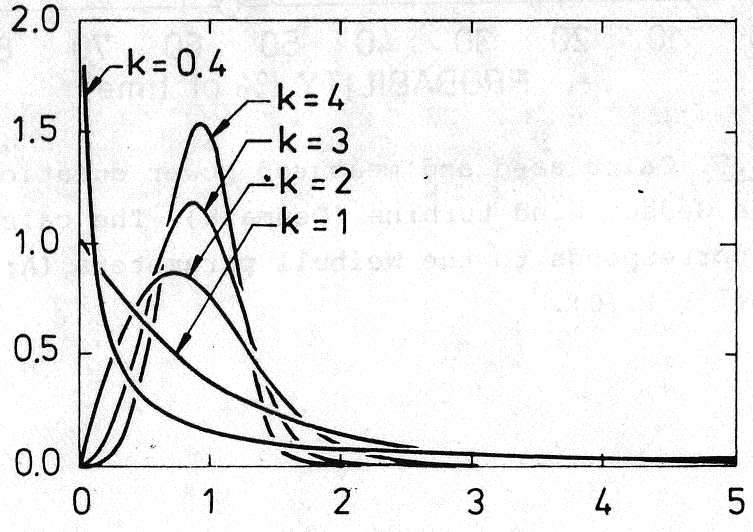

Fig. 4.1. The importance of the shape parameter k for the shape of the Weibull distribution.

The accumulated Weibull distribution F(u) which gives the probability of having a wind speed equal to or less than u is obtained by integrating Eq. (4.1) with the result

$$F(u) = 1 - \exp\left(-\left(\frac{u}{A}\right)k\right) \tag{4.2}$$

A special consequence of the Weibull distribution is that if u is Weibull distributed, so is u^m with parameters

$$\begin{aligned} A_m &= A^m \\ k_m &= \frac{k}{m} \end{aligned} \tag{4.3}$$

Some of the most important statistical quantities of the Weibull distributed variable u are listed below with the scale parameter inserted.

Mean value	$A\Gamma(1 + \frac{1}{k})$
Variance	$A^2[\Gamma(1 + \frac{2}{k}) - \Gamma^2(1 + \frac{1}{k})]$
Mean square	$A^2\Gamma(1 + \frac{2}{k})$
Mean cube	$A^3\Gamma(1 + \frac{3}{k})$
Mean energy	$\frac{1}{2}\rho A^3\Gamma(1 + \frac{3}{k})$
Modal value	$A(\frac{k-1}{k})^{1/k}$
Median value	$A(\ln 2)^{1/k}$

(4.4)

$u^m \cdot f(u)$ has its maximum for u equal to $A\left(\frac{k-1-m}{k}\right)^{1/k}$

4.2. Determination of the Weibull parameters

The determination of those values of the shape and scale parameters which give the best fit to a given set of observations given as a histogram can be performed by means of moment estimates and the use of a maximum likeness criteria. These concepts are briefly described in this section.

Maximum likeness

For the application of this method the data are first grouped in order to obtain a histogram and thereafter A and k are chosen so that the corresponding Weibull distribution has the best possible agreement with the histogram. For this a "maximum likeness" criterion (Barndorff-Nielsen, 1977) is applied. This criterion requires choosing the values of A and k to maximize the expression

$$\sum \hat{Pr}_i \ln(Pr_i(A,k)) \qquad (4.5)$$

where $Pr_i(A,k)$ is the theoretical probability density in the i'th interval, and $\hat{Pr}_i$ is the corresponding probability density derived from the observations.

It can be shown that maximizing Eq. (4.5) corresponds to minimizing

$$\sum Pr_i \ln \frac{\hat{Pr}_i}{Pr_i(A,k)} \qquad (4.6)$$

The determination of maximum likeness estimates for A and k is carried out numerically on a computer using an iterative algorithm. The calculations are initiated by making a guess for A and k. This guess is then based on estimates of the moments.

Estimates of the moments

The mean and mean cube values in the Weibull distribution are given by Eq. (4.4).

Defining

$$X_1(k) = \Gamma(1 + \tfrac{3}{k})\ \Gamma^{-3}(1 + \tfrac{1}{k})$$
$$X_3(k) = \Gamma^2(1 + \tfrac{1}{k})\ \Gamma^{-1}(1 + \tfrac{3}{k}) \qquad (4.7)$$

leads immediately to the following equations for k and A

$$X_1(k) = \frac{\overline{u^3}}{\bar{u}^3} \qquad (4.8)$$

$$A = \frac{\overline{u^3}}{\bar{u}^2} X_3(k)$$

The moment estimates for $\bar{u}$ and $\overline{u^3}$ are calculated from the set of observations by

$$\bar{u} = \frac{1}{N} \sum_i^N u_i$$
$$\overline{u^3} = \frac{1}{N} \sum_i^N u_i^3 \qquad (4.9)$$

Use of these estimates in Eq. (4.8) yields a set of equations which can easily be solved iteratively to obtain "moment estimates" for A and k.

Calculation procedure

In the practical calculations the moment estimates are calculated first. From these the starting values for maximum likeness parameters are chosen and an iterative solution is initiated. The iterative procedure is stopped when the relative change of the parameters becomes less than a certain percentage, say 1%.

4.3. Diurnal variation, yearly variation and calms

Most wind speed records from heights below 100 metres will show a pronounced diurnal and yearly variation. If the various wind regimes corresponding to nighttime and daytime conditions and/or the seasons are very much different it can be advantageous to divide the series with respect to these regimes before estimating the distribution function. Hence for example by estimating the Weibull parameters corresponding to day and night. One such procedure is described in Rejkoort and Wieringa (1983).

A problem that needs special attention is that of the recorded occurrence of calms. Such periods can be defined as periods where the wind speed is below a threshold wind speed u_T which is somewhere between 0.5 ms^{-1} and 2 ms^{-1} dependent either on the skill of the observer or the performance of a specific anemometer.

When a Weibull distribution is estimated from a data series with a high frequency of calms the fitting procedure most likely will produce a distribution with a k close to one, i.e. an exponential distribution. This is usually not a good approximation to the distribution of wind speed data in the frequency range, relevant for wind energy production.

For the estimation of the distribution function in such cases over the whole frequency range, a three-parameter function would often give a better fit than the Weibull function. However, what is wanted from an analysis of the specific series at hand is really not the best fit for that series but rather a statistical basis for estimating the mean wind statistics at various places in the region where the series was obtained. Hence to use the series for performing horizontal and vertical extrapolation. For that purpose we suggest that the problem of fitting a distribution to a data set with a high percentage of calms is circumvented in a very simple manner, namely by removing the calms from the data and keeping the percentage of removed observations as an additional parameter to the two Weibull parameters. Two examples will show the procedure.

Example 4.1

Figure 4.2 shows a histogram obtained from wind speed data from Mombasa Airport, Kenya. Hourly readings from an anemometer placed at the height of 2 metres in the period 1957-71.

As is evident there is a high frequency of wind speeds below 1 kt. Estimation of a Weibull function yields the shown exponential type curve with a k close to one. Figure 4.2 also shows the result when the calms are removed before the fit. The resulting Weibull function with a k equal 2.3 fits the distribution reasonable well in the relevant wind speed range. The estimated parameters for the data are: A = 5.1 kt, k = 2.30, freq(u < 1 kt) = 21.5%.

Example 4.2

Figure 4.3 follows the procedure as in the example above. The data are from Station Nord in Greenland (81°36'N, 16°40'W) measured at the height of 10 metres and reported every 3 hours (Hedegaard, 1983). Again it is seen that removing the calms before estimating the Weibull parameters results in an increase in the shape parameters from approximately 1 to 2. The estimated parameters for the data are: A = 5.0 ms^{-1}, k = 1.84, freq(u < 0.5 ms^{-1}) = 26%.

Note that there is a small error in the procedure because in addition to the percentages of calms ($u < u_T$; T = 0.5 ms^{-1} in the examples) which goes into the third parameter the Weibull function itself gives a certain frequency for $u < u_T$. Hence the parametric representations in the two examples give a higher frequency of calms than is actually observed. In the examples the error is less than 1%. However, if A and/or k are small a correction has to be made. Usually only one more calculation is necessary. If (obs) is the frequency of observed calms and f(calms) is the frequency of calms not accounted for by the fitted Weibull distribution we have:

$$f(\text{calms}) = f(\text{obs}) - (1-f(\text{obs}))(1-\exp\left(-\frac{u_T}{A}\right)k) \qquad (4.9)$$

which should be fulfilled within a few percent. Actually for wind energy purpose we are not really interested in the distribution of the probability mass for wind speeds below 5 ms^{-1} as was discussed in the previous chapter, but it is important for estimating the right shape of the function for wind speeds above 5 ms^{-1}.

4.4. Global variation of the Weibull parameter k

It is not possible to give a general rule for the variation of the Weibull k parameter with respect to latitude and altitude. This for the reason as discussed in the main part of this report that the wind speed is strongly influenced by local topography, vegetation, structures, and surface heating properties. It is sometimes claimed that k is close to one in the Arctic regions and near Equator. However, as follows from the two examples above this is probably due to the frequent occurrence of calms in these regions combined with attempts to fit the Weibull distribution over the full range of wind speeds. In general k will be in the interval from 1.5 to 2.5. For regions with very persistent winds like the trade winds k can be as large as 3 or more. Figure 4.4 shows such an example from the Cape Verde Islands (14°N, 24°W). Data from temperate latitudes often have k's close to 2.

In summary if data are not available for estimating k, a reasonable guess will often be k equal to two, i.e. the distribution will be estimated as a Rayleigh distribution.

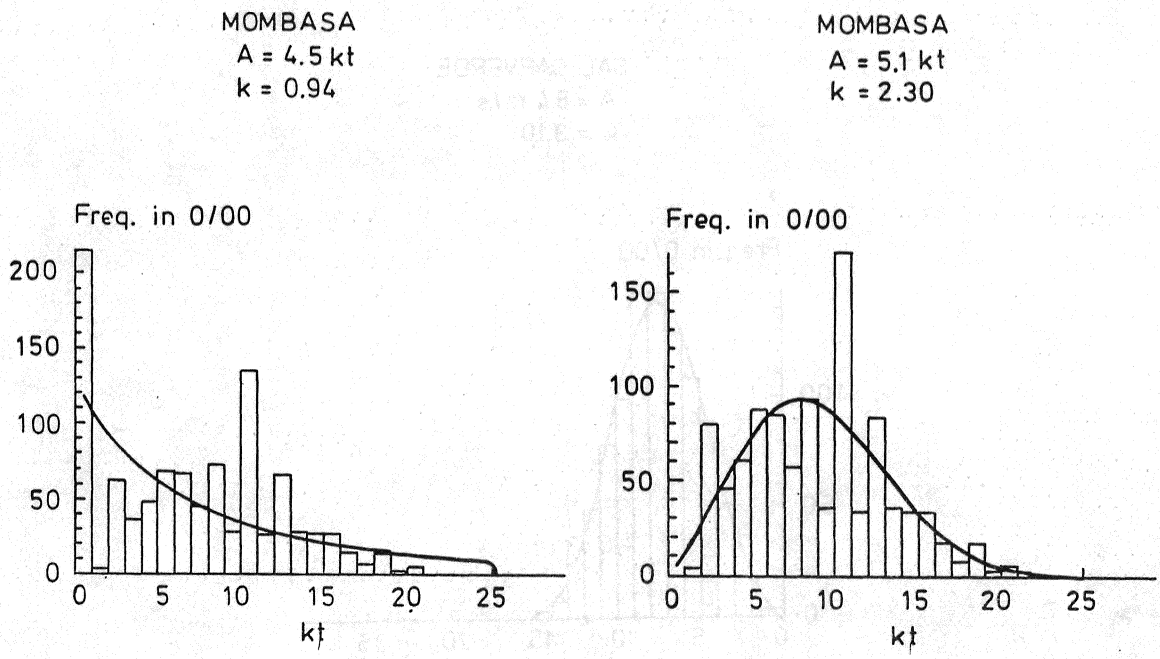

Fig. 4.2. Observed frequencies of occurrence of the wind speed at Mombasa Airport at 2 metres, 1957-71. The estimated Weibull distribution is shown as a continuous curve. Right figure is inclusive calms and left figure exclusive calms. (Data courtesy of the Meteorological Institute of Kenya).

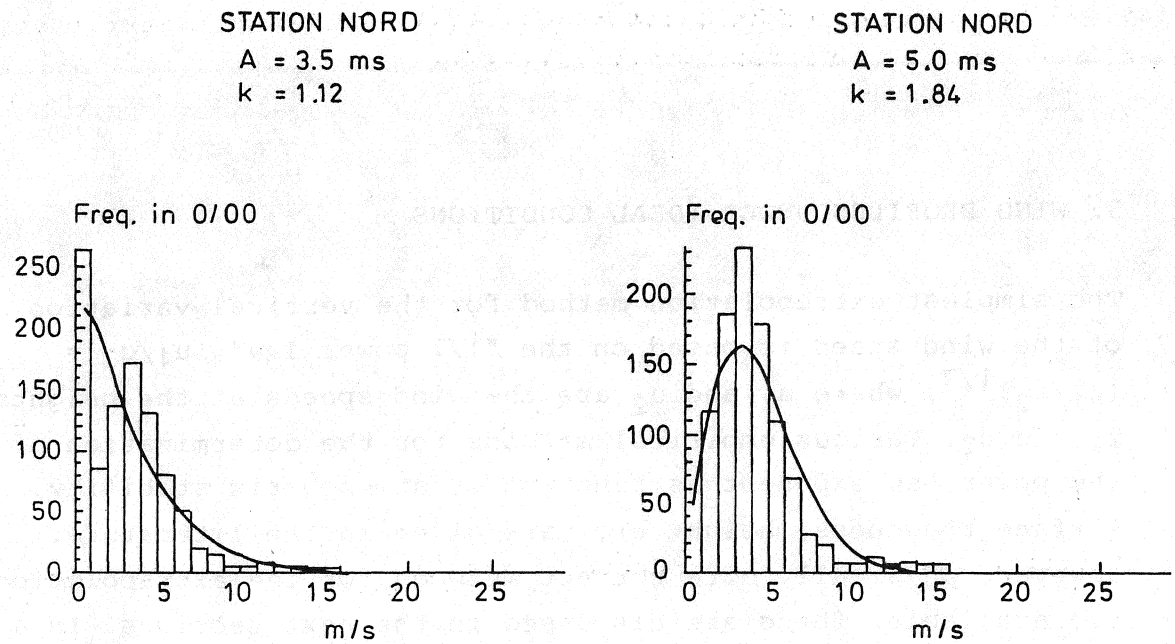

Fig. 4.3. Same as Fig. 4.2 but for Station Nord, Greenland, 10 metres height, 1962-72. Data from Hedegård (1983).

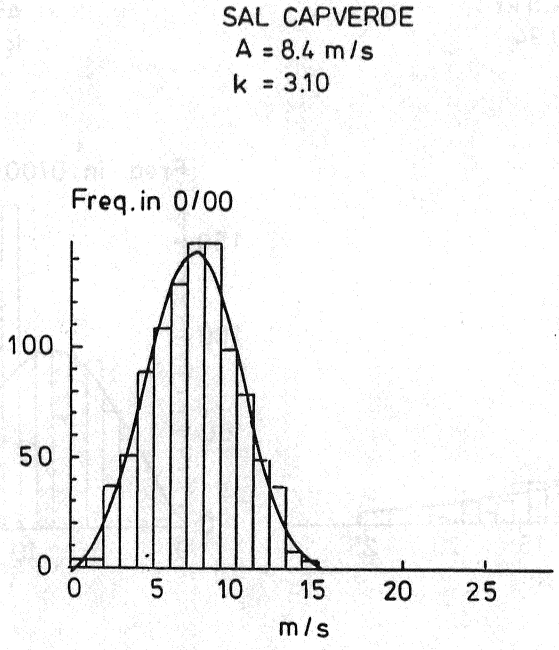

Fig. 4.4. Observed frequencies of occurrence of the wind speed at Sal Airport, Cape Verde, 10 metres height, 1978. The estimated Weibull distribution is shown as a continuous curve. (Data courtesy of the Meteorological Institute of Cape Verde).

5. WIND PROFILES UNDER IDEAL CONDITIONS

The simplest extrapolation method for the vertical variation of the wind speed is based on the "1/7 power law", $u_1/u_2 = (z_1/z_2)^{1/7}$, where u_1 and u_2 are the wind speeds at the heights z_1 and z_2. Various empirical methods for the determination of the power law exponent as function of atmospheric stability, surface roughness, height etc. are given in the literature. However, physically more correct methods for the extrapolation are available. These are discussed in the next sections. In a final section, we mention the geostrophic drag law, or what is known about the integral property of the planetary boundary layer.

5.1. The neutral surface layer

Under neutral, horizontally homogeneous conditions the familiar logarithmic wind profile

$$\bar{u} = \frac{u_*}{k} \ln \frac{z}{z_o} \qquad (5.1)$$

is valid near the surface, and up to heights of approximately 100 m (Panofsky, 1973). In Eq. (5.1) u_* is the so-called friction velocity which relates to the wind stress at the surface (Lumley and Panofsky, 1964), and k is a dimensionless constant, z is the height above ground, and z_o is the surface roughness length.

From profile analysis u_* and z_o are determined by plotting u versus the logarithm of z, determining the slope (u_*/k) and the intercept with u = 0 (which determines $\ln z_o$). Under certain conditions it is necessary to introduce a zero displacement height (shift in origin of z from the actual ground) when z_o happens to be small relative to actual roughness elements (for example at small heights above a forest). Typical values of z_o for a range of different natural surfaces are given in Fig. 5.1.

Alternative methods of determination of u_* is by turbulence measurements (eddy correlation, Lumley and Panofsky, 1964) or by direct measurement of the surface drag (Lynch and Bradley, 1974).

The requirement to the conditions for horizontal homogeneity is that advection should be small compared to other terms in the equations of motion. Thus comparing $u\partial e/\partial x$ with the local production of turbulent kinetic energy, e, leads to the condition $z/x << u_*/\bar{u}$ which is typically fulfilled for height to fetch ratios of 1/100. Requirements to stationarity can be considered analogously. In general it is sufficient if the relative change of windspeed $\Delta\bar{u}/\bar{u}$ satisfies $\Delta\bar{u}/\bar{u} << 1$.

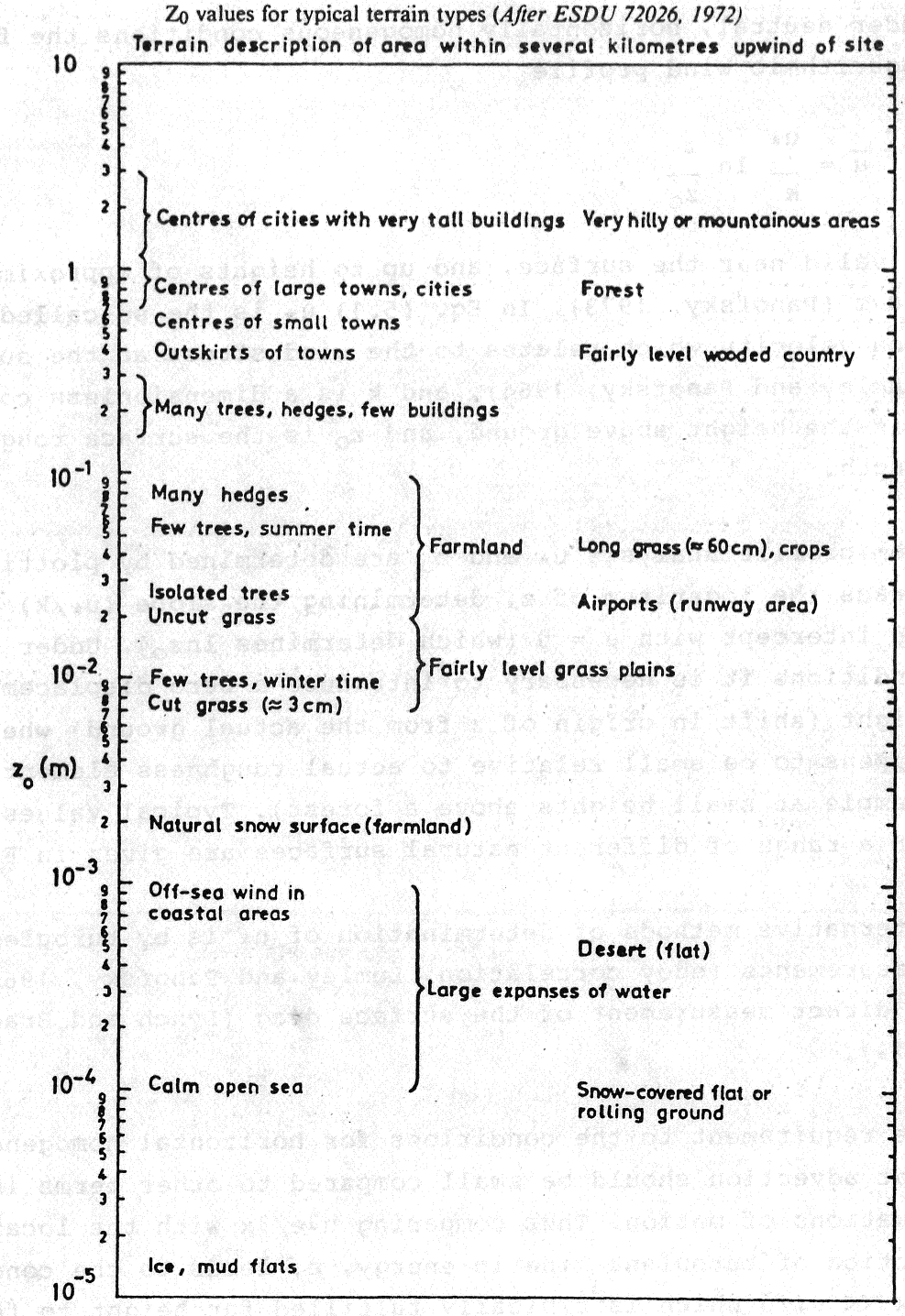

Fig. 5.1. ESDU 72026 1972 Summary of z_o values for different types of surfaces which can be used when applying Eq. (5.1).

5.2. The non-neutral surface layer

Under non-neutral conditions, which may be defined as situations where buoyancy production of turbulence is more than a few percent of the shear production, Eq. (5.1) must be corrected accordingly.

For such conditions the similarity theory of Monin and Obukhov (1954), which has substantial support from experimental work (Businger et al., 1971, Dyer and Bradley, 1982), is followed:

$$\bar{u} = \frac{u_*}{k}\left(\ln \frac{z}{z_o} - \psi\left(\frac{z}{L}\right)\right) \tag{5.2}$$

where ψ is a function which corrects for the influence of temperature stratification. L is the so-called Monin-Obukhov length, which is the height at which buoyancy production becomes of the order of the shear production of turbulence.

From Businger (1973) the following empirical expressions can be derived:

$$\psi = \begin{cases} \ln \dfrac{(x+1)^2(x^2+1)}{8} + 2 \operatorname{Arctan} \dfrac{1-x}{1+x}, & L < 0 \\ -4.7 \dfrac{z}{L}, & L > 0 \end{cases} \tag{5.3}$$

where for the unstable case x is defined as $x = (1-16\ z/L)^{1/4}$.

It is a bit unfortunate that the mathematical form of ψ in the unstable case is so complicated. The reason is that the empirical curve fit was done on its differentiated form, which characteristically enough then happens to be a relatively simple power law. A convenient close approximation for the unstable case is

$$\psi = \left(1 - 16 \frac{z}{L}\right)^{1/4} - 1 \tag{5.4}$$

which herewith is recommended.

Similar expressions as Eqs. (5.2) and (5.3) regarding the temperature profile near the ground are available (Businger, 1973). In this connection they are of less importance, except that they could aid in determination of L, and thereby in the vertical extrapolation of wind speed. A simple iterative procedure goes as follows:

For a set of measured values of wind and temperature (or temperature difference if the surface temperature is not known), the profile equations are solved for u_* and the equivalent temperature scale, θ_*, assuming that $|L| = \infty$ (i.e. neutral conditions). The obtained values are used to calculate an estimate of L according to its definition. With this value new estimates of u_* and θ_* are obtained from the profile equations leading to a refined value of L, and so on. The convergence is usually quite good, except under extreme stability conditions, and only a few of the above cycles are necessary. Louis (1979) has presented an explicit scheme which can be applied in the case where wind speed and temperature are available at one atmospheric level.

If the site is sufficiently homogeneous, it is even possible to iterate and calculate L from measurements of wind speed alone from a minimum of two different measurement levels, assuming that the surface roughness is known (Lo, 1979).

An example of wind profiles under various stability conditions are shown in Fig. 5.2. Note the large difference in the wind speed say at 10 m according to whether the conditions are stable or unstable. More than a factor of two variation is easily obtainable even though the geostrophic wind and the surface roughness are held fixed.

For routine application, where profiles are not available, let alone direct measurements of the relevant turbulent fluxes, a method suitable for use in connection with standard one-level observations where cloud cover is also available has been proposed. The basis is the following:

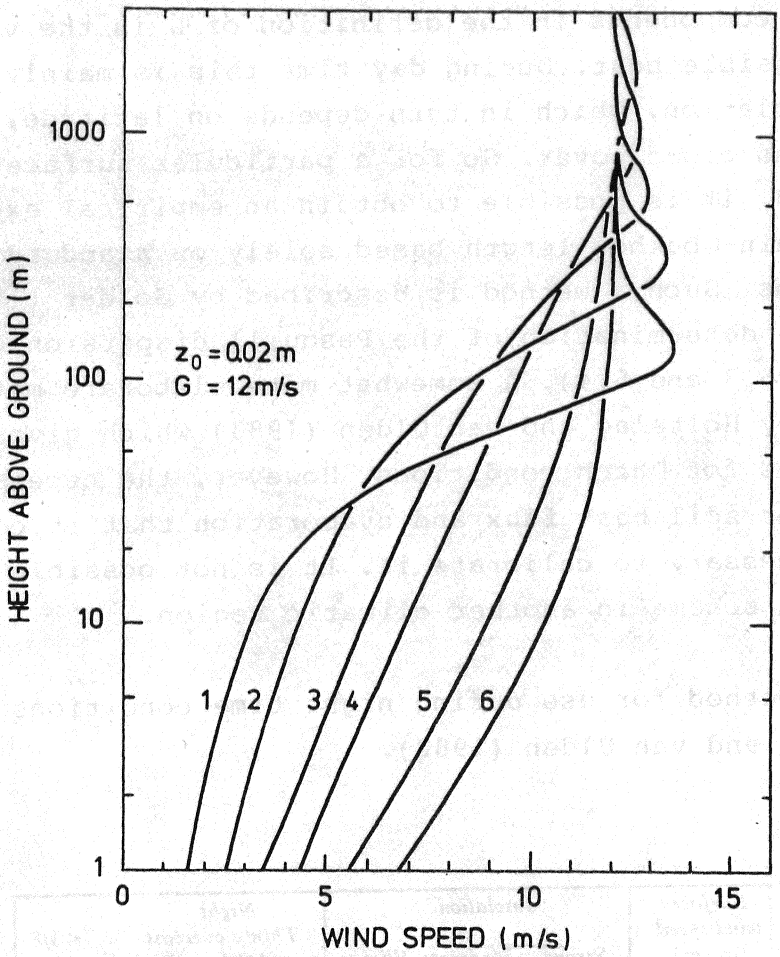

Fig. 5.2. Results from a one-dimensional numerical model incorporating the surface layer description Eq. (5.3). The result from the computation with this model is the cross isobaric angle α, the friction velocity u_*, and the wind profile. The inputs are the "external parameters z_o, G, L and the Coriolis parameter f, which in this case is equal to $1.2 \cdot 10^{-4}$ s^{-1}. The key to the numbers on the figure is given in the table below.

		L[m]	u_* [m/s]
1	Strongly stable	35	0.17
2	Stable	200	0.26
3	Near neutral	1000	0.37
4	Neutral	∞	0.44
5	Unstable	-400	0.57
6	Strongly unstable	-100	0.70

One of the components in the definition of L is the vertical flux of sensible heat. During day time this is mainly controlled by the insolation, which in turn depends on latitude, time of the day, and cloud cover. So for a particular surface, say a grass field, it is possible to obtain an empirical expression for the Monin-Obukhov length based solely on standard synoptic observations. Such a method is described by Golder (1972). It is based on determination of the Pasquill dispersion categories (see Figs. 5.3 and 5.4). A somewhat more elaborate method is described by Holtslag and van Ulden (1983) which gives quite good results for Dutch conditions. However, the necessary corrections for soil heat flux and evaporation that it contains make it necessary to calibrate it. It is not possible simply to apply their scheme in another climatic region.

A similar method for use during night time conditions is given by Holtslag and van Ulden (1982).

Surface wind speed (m/sec)	*Insolation*			*Night*	
	Strong	*Moderate*	*Slight*	*Thinly overcast or ≥ 4/8 low cloud*	*≤ 3/8 cloud*
< 2	A	A–B	B	—	—
2–3	A–B	B	C	E	F
3–5	B	B–C	C	D	E
5–6	C	C–D	D	D	D
> 6	C	D	D	D	D

Fig. 5.3. Pasquill's (1961) key to his stability categories. Strong insolation corresponds to sunny midday in midsummer in England, slight insolation to simialr conditions in midwinter. Night refers to the period from one hour before sunset to one hour after dawn. The neutral category D should also be used, regardless of wind speed, for overcast conditions during day or night, and for any sky conditions during the hour proceeding or following night as defined above.

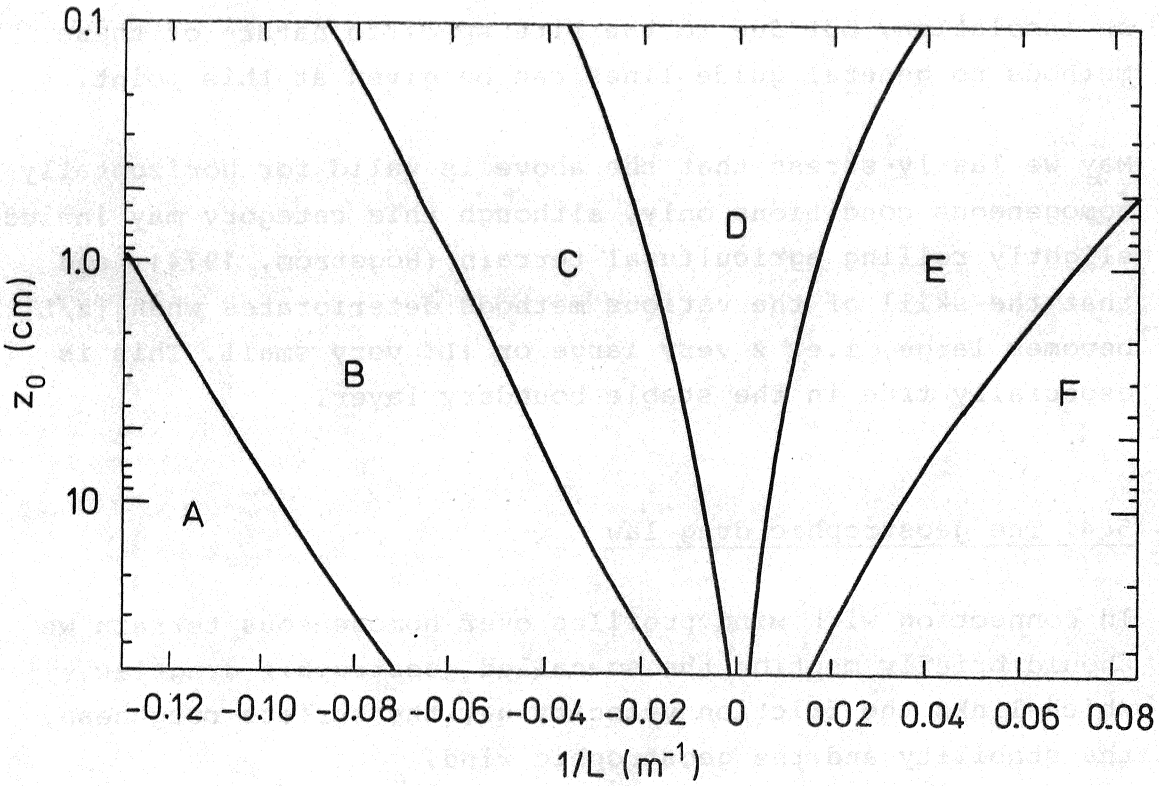

Fig. 5.4. Relationship between the Pasquill stability categories and the Monin-Obukhov length after Golder (1972). For a given set of conditions, it is seen that the rougher the surface the more the situation tends towards neutral.

5.3. Vertical extrapolation under ideal conditions

In summary, regarding vertical extrapolation of wind speed up to moderate heights, 50 to 100 m, this is possible using the logarithmic law (Eq. 5.2) with stability correction according to Eq. (5.3).

This is best done when profile information (i.e. a few observation levels) on wind and temperature is available. If this is not the case, estimates under neutral conditions can be obtained from a single anemometer, using an estimated value of the surface roughness (Fig. 5.1).

Under diabatic conditions a single anemometer level is also usable in connection with an empirical stability correction based

on insolation, but due to the site specific nature of these methods no general guide lines can be given at this point.

May we lastly stress that the above is valid for horizontally homogeneous conditions only, although this category may include slightly rolling agricultural terrain (Högström, 1974), and that the skill of the various methods deteriorates when $|z/L|$ becomes large, i.e. z very large or $|L|$ very small. This is especially true in the stable boundary layer.

5.4. The geostrophic drag law

In connection with wind profiles over homogeneous terrain we should briefly mention the so-called geostrophic drag law, which links the friction velocity u_*, the surface roughness, the stability and the geostrophic wind.

The subject has recently been reviewed in two WMO reports (WMO, 1979; 1981). The presentation here is only a short overview but presents an alternative treatment.

Ellison (1956) appears (as described in a recent paper by Krishna (1980)) to have been the first to give a solution to the stationary homogeneous equations of motion for the neutral planetary boundary layer using physically reasonable closure and boundary conditions: an eddy viscosity $K = k\, u_*\, z$ (one-layer model) and a logarithmic surface layer wind profile. His solution, which is analytical, can be written

$$\ln Ro + \ln \frac{u_*}{G} = \sqrt{\left(k \frac{G}{u_*}\right)^2 - B^2} + A \qquad (5.5)$$

$$\sin\alpha = -\frac{B}{k} \frac{u_*}{G} \qquad (5.6)$$

where A and B are universal constants. These expressions give the geostrophic drag u_*/G and the cross isobar angle α as functions of the surface Rossby number

$$Ro = \frac{G}{fz_o} \qquad (5.7)$$

as the only independent variable. This is the concept of Rossby number similarity, subsequently introduced by Lettau (1959).

Equations (5.5) and (5.6), which have later become known as the "drag laws" or the "Monin-Kazanski relations", were rederived (by Blackadar and Tennekes, 1968, and others) in a very elegant fashion without using any direct assumptions regarding the eddy viscosity, but by way of so-called asymptotic matching. A crucial finding of these matching theories is that the relevant scale height of the boundary layer is of order u_*/f. However, this was also part of Ellison's solution. A further result of this early work was a theoretical determination of the constants A and B:

$$A = 2\gamma - \ln k = 2.07$$

$$B = \pi/2 = 1.57 \ ,$$

where $\gamma = 0.5772$ is Euler's constant. This is remarkably close to modern empirical evidence (to which we shall return below) suggesting $A \simeq 1$ and $B \simeq 5$ (with Ellison's A one would overestimate the drag by about 10% for typical atmospheric conditions, but, of course, the small value of B significantly underestimates the cross-isobar angle, a consequence of the continuing increase of K throughout the boundary layer).

A particularily simple approximation to the geostrophic drag law for neutral conditions was suggested by Jensen (1978) as

$$\frac{u_*}{G} = \frac{0.5}{\ln(Ro)}$$

Extension of the drag law to include diabatic conditions was probably first suggested by Zilitinkevich et al. (1967), where it was suggested that non-neutral conditions could be treated by letting A and B be functions of μ, where

$$\mu = \frac{u_*/f}{L} \qquad (5.8)$$

i.e. the ratio of the neutral boundary layer height and the Monin-Obukhov length. This was tested against experimental data by Zilitinkevich and Chalikov (1968) using the Great Plain data (Lettau and Davidson, 1957) taken at O'Neill, Nebraska, and by Clarke (1970) using data taken at Kerang and Hay in southern Australia. Unfortunately, the scatter of the data was very large, and when A and B were plotted versus μ, it was not surprising that the empirical curve fit to the data was quite different for the two investigations. This raised serious doubts about the μ-scaling. In a uniform reanalysis of the two data sets, Arya (1975) showed that this difference was an artifact, although the scatter remained.

For unstable conditions the numerical model of Deardorff (1970) and others suggested that the depth of the convective atmospheric boundary layer is independent of u_*/f and should be characterized by the height z_i of the capping inversion which always exists on top of the mixed layer. This leads to the suggestion (Deardorff, 1972) that z_i/L replace μ as the independent variable in the A and B functions. A formal derivation of this modified similarity theory was given by Zilitinkevich and Deardorff (1974). The choice between u_*/f and z_i cannot be based on theoretical grounds, but must rather rely on physical reasoning and empirical results to determine which produces the least scatter in the plots of data. In this respect the situation is inconclusive as the use of z_i-scaling did not reduce the scatter in the work of Arya (1975) mentioned above. In an analysis by Melgarejo and Deardorff (1974), also using Wangara data, the same conclusion was found.

It should be emphasized that the large difference between the empirical curves that have been published could be a result of the mostly arbitrary ways in which the curve fitting has been performed (lines drawn by eye; third order polynomial, etc.) rather than a result of fitting functions determined from similarity considerations of the limiting behaviour for large $|\mu|$.

The analysis of the Wangara data by Clarke and Hess (1974) does not suggest the use of z_i as the scaling height, but uses u_*/f for all stabilities. On the contrary they show (Clarke and Hess, 1973) that u_*/f is preferable unless $z_i < 0.25\ u_*/f$. A plot of their results for A and B is shown in Fig. 5.5.

They made an attempt to derive representative values of z_o and u_* for the experimental area by weighting profiles from two characteristic sites together. Cases with very low wind speeds were excluded (possible stopping of cup anemometers). Furthermore, the data were divided into 24 stability classes, based on μ, each class containing about 40 observations (one hour values). By this procedure, the effect of baroclinity would tend to be minimized. In briefly reverting to Ellison's model, which is able to include baroclinity, the qualitative effect of horizontal temperature gradients is to add to A and B a term which is proportional to a component of the thermal wind resolved in the direction of the surface wind. So because it is an additive effect and because it seems reasonable to assume that stability and horizontal temperature gradients are uncorrelated, the (potentially large) effect of baroclinity would disappear by averaging many cases.

A comparison of the analysis of Clarke and Hess with that of Arya reveals that the scatter in the latter has been considerably reduced, and that it is even possible to see the behaviour on the stable side, in agreement with theory and model results (see below).

The neutral barotropic values of A and B are of special interest. To calculate these values, Clarke and Hess selected data for $|\mu| \leq 10$ and at the same time rejected cases of rapid stability change. From a total of 52 hourly observations they found $A = 1.1 \pm 0.5$ and $B = 4.3 \pm 0.7$.

Revision of (or one could say a compromise between) the two similarity theories for the behaviour of the A and B functions in convective conditions has been indicated by recent modelling studies (Wyngaard et al., 1974 and others). They show that the parameter

$$\frac{u_*/f}{z_i} \tag{5.9}$$

should be included in the list, making the empirical determination of the A and B functions more difficult as it adds a second independent variable. This, together with the generally large scatter of experimental results, led Arya (1977) to suggest the use of A and B functions entirely based on model results (Deardorff, 1972; Wyngaard et al., 1974).

It is possible to obtain an estimate of the asymptotic behaviour of the A and B functions. Thus for strong stability, relatively simple scaling arguments give

$$B \propto \mu 1/2 \tag{5.10}$$

and subsequently

$$A \propto -\mu 1/2 \tag{5.11}$$

in qualitative agreement with numerical model results of Businger and Arya (1974) and Wyngaard (1975). For use over the entire range $0 \leq \mu < \infty$ a possible interpolation formula for stable conditions is

$$\left.\begin{aligned} A &= 1 - \mu 1/2 \\ B &= 5 + \mu 1/2 \end{aligned}\right\} \quad \mu = \frac{u_*/f}{L} > 0 \ , \tag{5.12}$$

where the neutral values 1 and 5 have been suggested in agreement with Clarke and Hess (1974). The relationships are depicted in Fig. 5.5.

For very unstable conditions, on the other hand, the shear would not be distributed over the depth of the boundary layer, but rather in a shallow layer near the ground. A depth of order -L is suggested. This leads to the drag law originally suggested by Gill (1968)

$$G = \frac{u_*}{k} \ln \frac{-L}{z_o} \quad , \tag{5.13}$$

The strong mixing thus keeps the wind profile flat above $z \sim -L$. In analogy, any Ekman turning of the wind will be prohibited in the boundary layer, and the adjustment of α to its proper value occur in the shallow inversion layer at the top of the convective boundary layer at height z_i. Integration from $z = 0$ to $z = z_i$ of the equation of motion, under this condition, reads $-G \sin(\alpha) z_i = u_*^2/f$ which combined with Eq. (5.6) gives

$$B = k \frac{u_*/f}{z_i} \tag{5.14}$$

This retrieves the parameter dependence suggested in (5.9). To estimate A under these convective conditions we note that if

$$z_i > \frac{G}{f} \left(\frac{k}{\ln(-L/z_o)} \right)^2 \tag{5.15}$$

which is almost always the case (in a quite extreme situation where G is small, say 5 m/s, the conditions very convective, say $-L = 10$ m, and the surface roughness, $z_o = 10$ cm, the criterion is met for $z_i > 400$ m) then B^2 in Eq. (5.5) can be negleted in comparison with $(kG/u_*)^2$, which leads to

$$A = \ln(-\mu) \tag{5.16}$$

In passing, we mention that z_i despite of its undisputed importance for various turbulent quantities, does not seem to be of any relevance in the drag law (logical in view of Eq. (5.13)) except for its influence through B on a small cross-isobaric angle.

In summary regarding the A function in unstable conditions, a possible interpolation formula would be

$$A = 1 + \ln(1-\mu) \quad , \quad \mu = \frac{u_*/f}{L} < 0 \tag{5.17}$$

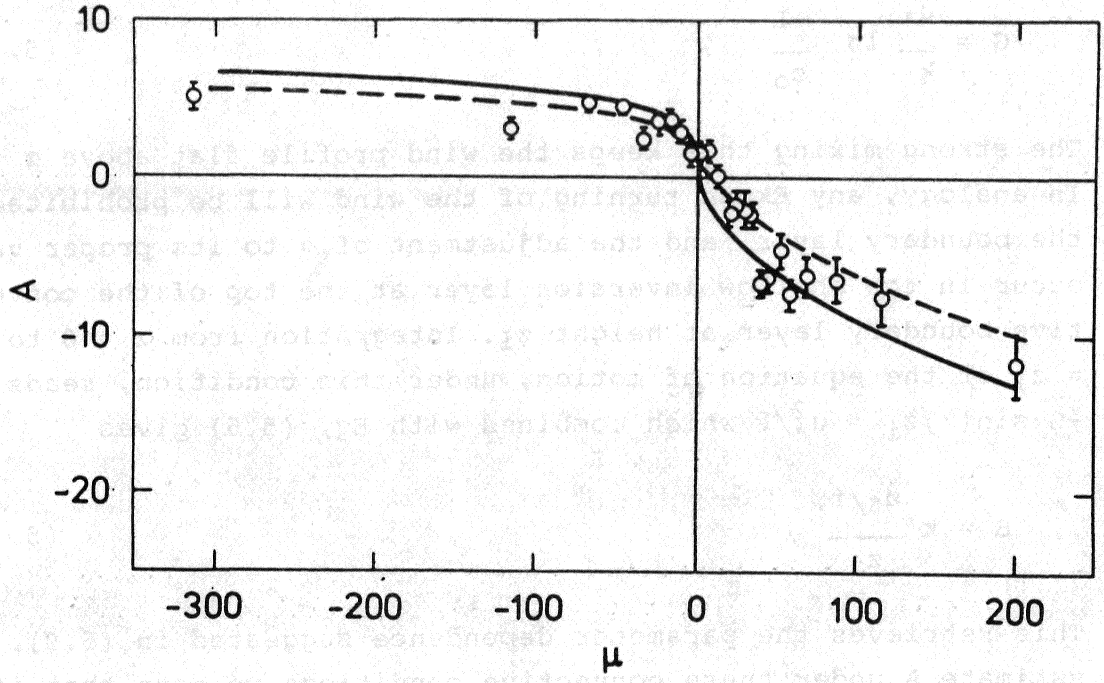

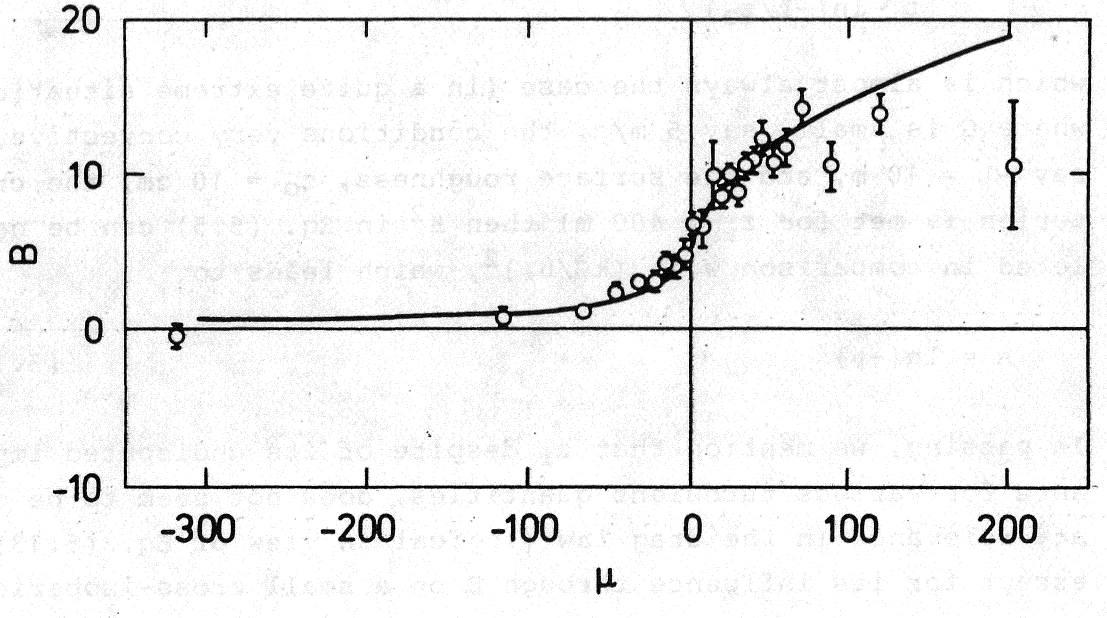

Fig. 5.5. Values of A(μ) and B(μ) evaluated from the Wangara data using surface geostrophic winds (Clarke and Hess, 1974). On the stable side, the expressions given in Eq. (5.12) are shown for comparison. On the unstable side, Eq. (5.17) for A and Eq. (5.19) for B (with $z_i >> u_*/f$ and a = 1/25) are given.

which fulfill both the neutral limit ($A \simeq 1$ for $\mu = 0$, Clarke and Hess, 1974) and the limit for very unstable conditions as required by Eq. (5.16).

A formula for B would have to fulfill an extra limit process. First consider the development above leading to Eq. (5.14), it is implicitly assumed that the boundary layer is limited by z_i, i.e. that z_i is smaller than the Ekman height or $z_i < u_*/f$. If this is not the case the integration should instead be performed over the interval $z = 0$ to $z = u_*/f$ which from Eq. (5.14) is seen to lead to

$$B \simeq k \tag{5.18}$$

An interpolation formula which will accommodate this is

$$B = \frac{5-k}{1-\mu a} + k \frac{u_*}{f} \left(\frac{1}{z_i} + \frac{1}{u_*/f} \right) \tag{5.19}$$

which fits in the various limits including Eqs. (5.14) and (5.18), except in a situation with a significant low inversion ($z_i < u_*/f$) under otherwise neutral conditions ($\mu = 0$). Equation (5.19) is shown in Fig. 5.5. In Eq. (5.19) a is a constant of order 1/25, the purpose of which is to make the transition from neutral ($B = 5$) to unstable conditions ($B = k + (ku_*/f)/z_i$) suitably smooth.

The above suggested interpolation expressions for $A(\mu)$ could possibly be improved by making them approach the neutral value with the same slope from both the stable and unstable side. In the preparation of a European Wind Atlas, which will be described further in Chapter 9, it was noticed that a straight forward application of Eqs. (5.12) and (5.17) gave spurious variations in the extrapolated geostrophic wind at hours around sunset and sunrise. An alternative expression

$$A = \begin{cases} A_o - (\mu + a)^{1/2} + a^{1/2} & \mu \geq 0 \\ A_o + \ln(b - \mu) - \ln b & \mu \leq 0 \end{cases}$$

with a = 5 and b determined such that A is differentiable in $\mu = 0$ essentially removed that daily variation in G. Another point noticed in this study was that a probably better choice of the neutral value of A is 1.8.

The geostrophic resistance law is based on the assumption of near geostrophic balance of the free flow. This condition cannot be met near the equator where f = 0. Theories for the tropical boundary layer similar in simplicity to the drag laws do not exist. When the Coriolis force becomes unimportant the time derivatives in the equations of motion will have to be taken into account. One simple approach based on K-theory was presented by Holton (1971). The conditions at low latitudes are still much less understood, however, in large extent also because of the lack of micrometeorological data.

6. PERTURBATIONS BY SIMPLE CHANGES IN SURFACE CONDITIONS

Downstream of a discontinuity in the surface conditions an internal boundary layer, IBL, develops. Above the IBL no change has been felt. In the classical treatment of the roughness change problem, the intermediate adjustment region is neglected and for example the wind profile is assumed to consist of two logarithmic sections, each adjusted to the respective regions, and joining in a kink at height H at the top of the IBL. Figure 6.1 gives an example of the wind profile at two different distances downstream of a smooth to rough transition. This simple model gives a fit to experimental data which is sufficiently good for practical application.

Traditionally this problem has been limited to neutral conditions. Using the principle of limited diffusion rate ($dH/dx \propto u_*/u$) the kink model results in (see f.ex. Jensen, 1978)

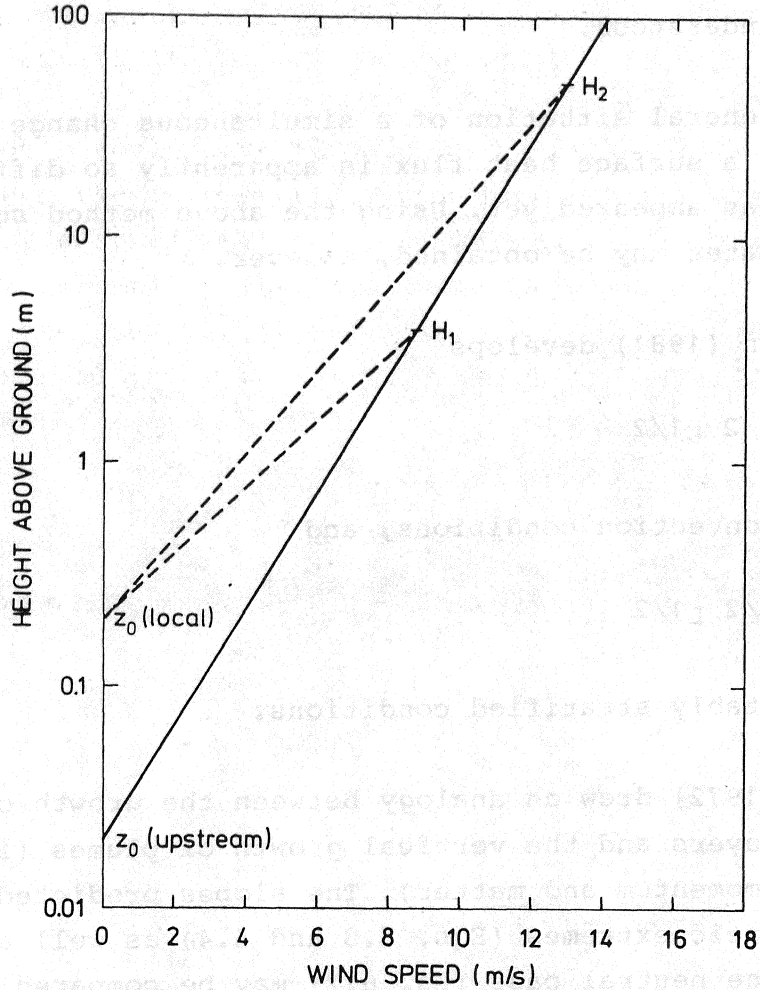

Fig. 6.1. The wind profile after a smooth to rough transition (from z_o = 2 cm to z_o = 20 cm) at two different distances downwind of the transition. The local profile (dotted line) joins the upstream profile at the height H determined from Eq. (6.2) with a ≈ 0.5. The height H_1 corresponds to a fetch of x = 20 m and H_2 to x = 500 m.

$$H \ln(H/z_o) \approx ax \qquad (6.1)$$

in which a is about 0.3 and x is the distance from the discontinuity. It is an empirical fact that this implicit equation is well approximated by the power law

$$H = a\, z_o^{1/5}\, x^{4/5} \qquad (6.2)$$

For non-neutral conditions the roughness change situation is not well understood.

The more general situation of a simultaneous change in roughness as well as a surface heat flux is apparently so difficult that no study has appeared yet. Using the above method some ball park estimates may be obtained, however.

Thus Jensen (1981) develops

$$H \propto x^{3/2}/L^{1/2} \qquad (6.3)$$

for free convection conditions, and

$$H \propto x^{1/2}\, L^{1/2} \qquad (6.4)$$

for very stably stratified conditions.

Pasquill (1972) drew an analogy between the growth of internal boundary layers and the vertical growth of plumes (i.e. diffusion of momentum and matter). The slopes predicted in the above diabatic extremes (Eqs. 6.3 and 6.4) as well as the result for the neutral case (Eq. 6.2) may be compared to the slopes of the Pasquill-Gifford curves (see Fig. 6.2).

The small roughness effect present in (6.2) does not enter in the diabatic extremes of (6.3) and (6.4). For moderate variations in stability, however, both L and z_o may enter the problem. In this range, a rational approach is to build on a formula derived by van Ulden (1978) for diffusion from a ground level source. This is done by using power-laws for u and the diffusivity K in the diffusion equation, solve for dH/dx (where H is taken as a measure of the depth of the plume at distance x), and then substitute proper Monin-Obukhov expressions for u and K back into the solution. The expression resulting from this, non-rigorous procedure may then be integrated to give H as a function of x.

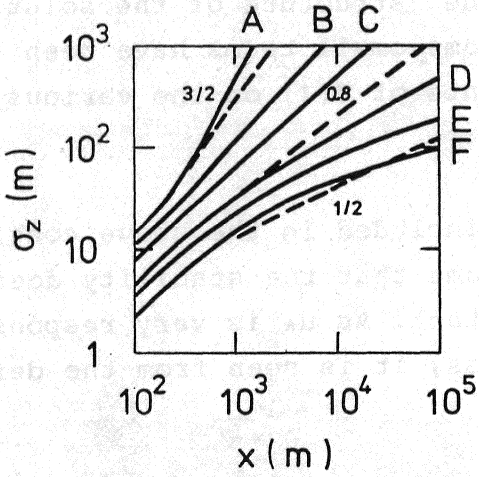

Fig. 6.2. The vertical standard deviation of a Gaussian plume under various stability conditions (A, B, ... F) as a function of distance from its source. (After Turner, 1967). The dashed lines correspond to Eqs. (6.2), (6.3), and (6.4).

This integration presents no difficulty in the stable case where $\psi(z/L)$ is linear in the argument (see Eq. 5.3), but for unstable conditions where ψ is a rather complicated function no analytical solution is possible. However, using the approximation given in Eq. (5.4), allows a solution. For this case as well as for the stable case the structure of the solution is closely approximated by

$$H(\ln(H/z_o) - 1 - \psi(H/L))\ \phi(H/L) \simeq ax \qquad (6.5)$$

which is seen to be compatible with the neutral solution Eq. (6.1). Referring back to Chapter 5 the empirical fit of Businger et al. gives

$$\phi = \begin{cases} \left(1 - 16\,\frac{H}{L}\right)^{-1/4}, & L < 0 \\ 1 + 4.7\,\frac{H}{L}, & L > 0 \end{cases} \qquad (6.6)$$

When it is said that the "structure of the solution approximates" it means that some small terms have been thrown and the proportionality constants of O(1) on the various terms have been adjusted to unity.

Although heat flux is included in the above considerations, these developments assume that the stability does not change, or that L(x) is a constant. As u_* is very responsive to changes in the surface roughness, it is seen from the definition of L

$$L = - \frac{u_*^2 T}{kg\theta_*} \tag{6.7}$$

that this constancy requires a rather specific downwind variation in surface heat flux, ($\equiv \theta_* u_*$) which contrasts the more general diabatic roughness-change situation in which it is expected that both u_* and θ_* change in such a way that L(x) is not constant. Furthermore, in a case where the stability changes from stable to unstable, the development of the IBL is no longer diffusion rate limited, but constrained by the entrainment in analogy with the daytime mixed layer. Thus

$$H \simeq \left(\frac{\theta_* u_* x}{\gamma u} \right)^{1/2} \tag{6.8}$$

where γ is the value of the stable lapse rate of the potential temperature above the IBL.

For the present purpose it is assumed that Eq. (6.5) can be used with sufficient accuracy, noting that we are concerned with moderate to high wind speeds at which extreme stabilities are infrequent.

7. PERTURBATIONS BY LOW TERRAIN FEATURES

Topographic features such as hills, valleys, cliffs, escarpments, or ridges, affect the wind speed. Near the summits or crests of these features the wind will be accelerated, while near the foot and in valleys it will be decelerated.

Evidence from theoretical work (Jackson and Hunt, 1975) and from numerical models (Taylor and Gent, 1974) as well as from experimental observations (Peterson et al., 1976) all show relatively large flow perturbations when the surface change elevation. Thus Peterson et al. (1976) state that the effect on the flow of a gradual surface elevation change of 2 m over 50 m, downwind of a shore line, is far larger than the effect of a simultaneous roughness change of approximately three orders of magnitude. The profile from their measuring mast just on top of the "escarpment" still resembles that of the change-of-roughness case, i.e. a kink is apparent, but in addition the upper part of the profile has greater wind speeds than the upstream profile at the same relative elevation. Terrain features of sufficient steepness will even cause the speeding-up of a sheet of intermediate fluid to velocities exceeding those of upper layers. Thus a low-level jet may develop locally.

The magnitude of this overspeeding, as well as the height at which it occurs can be qualitatively described using the analytical theory of Jackson and Hunt (1975).

Before going into further detail about this it is timely to warn against use of the old "escarpment rule" according to which the wind speed above a topographic feature is supposed to be equal to the speed upstream at the same horizontal level. This is inaccurate and misleading.

Figure 7.1 shows some preliminary data from a recent experiment. The hill is about 100 m high, so the "escarpment rule" would in

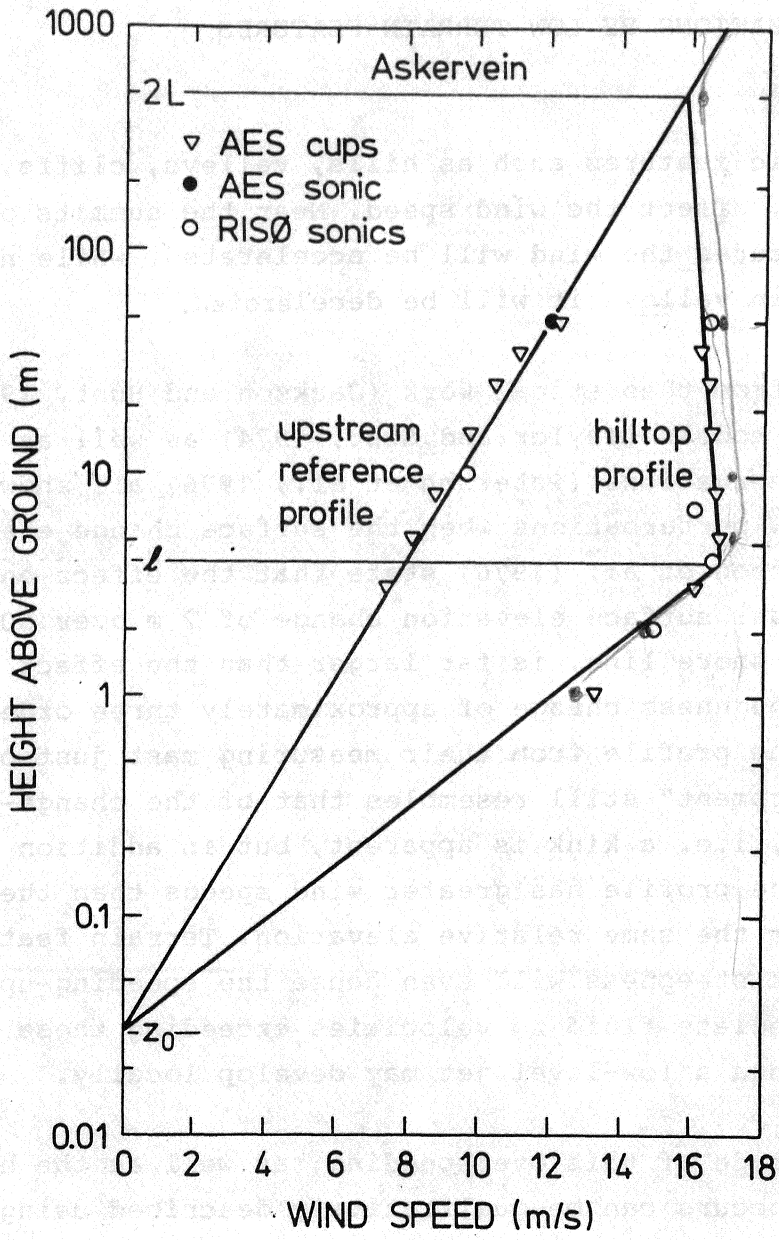

Fig. 7.1. Simultaneously recorded wind profiles (October 3, 1983, 14.30 to 15.30 local time) upstream and on the top of the hill Askervein on the Isle of South Uist on the Hebredies, during a recent international field experiment with participants from Canada, Denmark, F.R. Germany, New Zealand and United Kingdom. Background and details of the experiment are given in Taylor and Teunissen (1983).

this case give a wind speed of about 13 m/s on the hill, somewhat less than the observed 17 m/s. However, in a different case, the result could be the other way around. This is because the perturbation in addition to the height also depends on the horizontal length scale of the terrain feature in question. Furthermore, as we shall see below, the perturbation that occurs must be computed relative to conditions at the same level above local ground.

The analytical solution presented by Jackson and Hunt (1975) for the perturbation to flow in a turbulent boundary layer by change in surface elevation (two dimensional, i.e. a change along the direction of the wind only) consists of two layers which are made to overlap in a fuzzy zone at height ℓ. In the "outer layer" above ℓ the speed-up caused by a hill is treated as an inviced phenomenon. Because of this speed-up, an enhanced shear and thereby turbulence production is set up in the inner layer below ℓ. By matching the two layers, the velocity perturbation $\Delta u(z)$ in the outer layer, relative to the undisturbed upstream wind speed $u(z)$ at the same height, becomes

$$\Delta s(x,z) = \sigma(x,z) \frac{h}{L} \frac{\ln\left(\frac{L}{z_o}\right)}{\ln\left(\frac{\ell}{z_o}\right)} , \qquad (7.1)$$

where σ is a function that depends on the integrated slope of the terrain feature (but not on the actual h, length L or slope h/L). Jackson (1979) has provided solutions for σ, for some terrain shapes. Two typical ones are given in Fig. 7.2, one for a ridge and one for an escarpment. Other mathematical forms or "terrain shapes" will give slightly different answers. It has to be noted that the conventional definition of L for a hill is only half of that given in Fig. 7.2a. Below we shall refer to that particular L as the "quarter length".

HILLSHAPES AND SOLUTIONS

Triangular Ridge

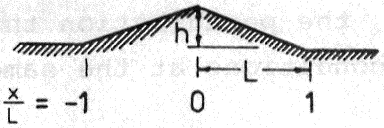

$$\sigma(x,z) = \frac{1}{2\pi} \ln \frac{[(\frac{x}{L}-1)^2 + (\frac{z}{L})^2][(\frac{x}{L}+1)^2 + (\frac{z}{L})^2]}{[(\frac{x}{L})^2 + (\frac{z}{L})^2]^2}$$

Triangular Ramp

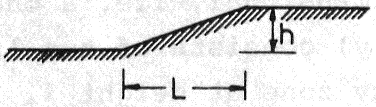

$$\sigma(x,z) = \frac{1}{2\pi} \ln \frac{(\frac{x}{L}+\frac{1}{2})^2 + (\frac{z}{L})^2}{(\frac{x}{L}-\frac{1}{2})^2 + (\frac{z}{L})^2}$$

Fig. 7.2. Hill shapes and solutions for $\sigma(x,z)$ (Jackson, 1979).

7.1. Ridges

In Eq. (7.1) let us first analyze the parenthesis on the r.h.s.: According to Jacksom and Hunt (1975) the depth of the inner layer is given by

$$\ell \ln(\ell/z_o) \simeq 2k^2 L \ , \qquad (7.2)$$

but for the range of values of ℓ/z_o which are relevant this implicit expression may be approximated by the power-law expression

$$\ell/z_o = a(L/z_o)^{0.8} \qquad (7.3)$$

where a is supposed to be ~0.3 when L is the quarter length. This particular part of their solution is not very appropriate. In the example in Fig. 7.1 for example the value of ℓ would be 13 m. If it was not for other examples (e.g. Bradley, 1983) it could be a matter of the value of the constant a. Alternative arguments give

$$\ell(\ln(\ell/z_o))^2 \sim L \ , \tag{7.4}$$

which with the above power-law approximation give the equivalent

$$\ell/z_o = b(L/z_o)^{0.67} \ , \tag{7.5}$$

which with b = 0.3 does a better job than Eq. (7.3) in matching the observations made over the L/z_o range encountered in nature. Anyway, whatever the power is, one finds

$$\frac{\ln(L/z_o)}{\ln(\ell/z_o)} \cong \frac{1}{x} \tag{7.6}$$

where x is the power, and where it has been assumed that $\ln(L/z_o) >> 1$.

Regarding the σ-function in Eq. (7.1), referring to Fig. 7.2a, let us evaluate it at the height ℓ at the crest of the ridge (the expression is not valid below ℓ since it represents an outer layer solution). As $(\ell/L) << 1$ we get $\sigma \cong (2\pi)^{-1} \ln(L/\ell)^4$ or

$$\sigma = 2/\pi \ln(L/\ell) \tag{7.7}$$

which by means of an expression of the form of Eq. (7.3) or (7.5) transforms to

$$\sigma \cong \frac{2}{\pi}\left[(1-x) \ln \frac{L}{z_o} - \ln b\right] \ , \quad b \simeq 0.3 \tag{7.8}$$

which is seen to be rather constant as it only varies as a slow function of L/z_o: over an extreme variation of L from say 50 m to 1000 m and of z_o from 1 cm to 50 cm, σ from Eq. (7.8) only varies from about 2 to 3. The point of the above is that both the above factor and the factor $\ln(L/z_o)/\ln(\ell/z_o)$ is relatively constant whereby Eq. (7.1) may be approximated by

$$\Delta s \cong c \frac{h}{L} , \qquad (7.9)$$

giving the relative speed-up at the crest of the hill, at a height above the ground given by Eq. (7.5). The above developments suggest c = 2/0.67 to 3/0.67 or 3 to 4.5, depending on the size of L/z_o. For L according to the quarter length definition this corresponds to c ≅ 2 in agreement with experimental evidence.

Below ℓ, theoretical arguments indicate that the perturbed profile is logarithmic. This is a rather neat result from the point of view of giving a simple rule of construction of wind profiles over topography. Thus Jensen and Peterson (1978) suggest in analogy with the simple roughness-change profile, to seek a similar representation, only that this case requires two kinks. The double kink profile then consists of (1) a section below ℓ with increased shear, (2) an intermediate steep section and (3) a section above the upper kink where the profile is not influenced. In reality, of course, the kinks are not sharp corners but smooth transitions.

The gross shape of the profile above a hill is thus determined by three variables: (a) the degree of speed-up over the feature (h/L); (b) the height of the lower kink which depends on L/z_o; and (c) the height of the upper kink, which under neutral conditions may be assumed to be of order L (pressure perturbation argument). An example of a profile constructed along these lines is shown in Fig. 7.1 with c in Eq. (7.9) equal to 2.15 (the quarter length L = 250 m) and the height of the upper kink at z = 2L. The agreement with the measured data is seen to be rather good.

Even though the formulae are strictly valid for two dimensional conditions they tend to give fair result for more general cases, i.e. oblique flow over a ridge (where the wind speed to be considered is now the perpendicular component), and even in cases of common three-dimensional hills.

7.2. Escarpments

The flow perturbation caused by escarpments may be treated in the same way as above. For a ramp-like feature Fig. 7.2b gives a formula for σ to be used in Eq. (7.1).

It is also here possible to simplify. At the top of the escarpment we get $\sigma \cong (2\pi)^{-1} \ln(1+(L/\ell)^2)$ or since $\ell << L$

$$\sigma \cong \frac{1}{\pi} \ln \frac{L}{\ell} , \qquad (7.10)$$

which is precisely half of that for a ridge or hill (compare Eq. 7.7). We note again that ℓ is the lowest height at which the σ-expression is allowed to be evaluated.

The suggestion of how to construct a wind profile on top of an escarpment is completely analogous to the ridge or hill case in the previous section, but less experimental evidence support the suggestion.

However, it is known that away from the point of maximum speed-up the above formula does not give an entirely satisfactory explanation of observed flow perturbations as they fail to predict correctly the vertical and downwind variation of the velocity perturbation (Jensen, 1983).

Regarding the vertical extrapolation at the top of the escarpment, and at the symmetrical point at the foot, comparison with data seen to indicate that the vertical extend of the perturbation is larger, respectively smaller than in theory (see Fig. 7.3).

Regarding the downwind variation of the speed-up, it is noted from Fig. 7.2 that for large distances $x >> L$ ($>> z$), the expression for σ reduces to

$$\sigma = \frac{1}{\pi} \frac{L}{x} , \qquad (7.11)$$

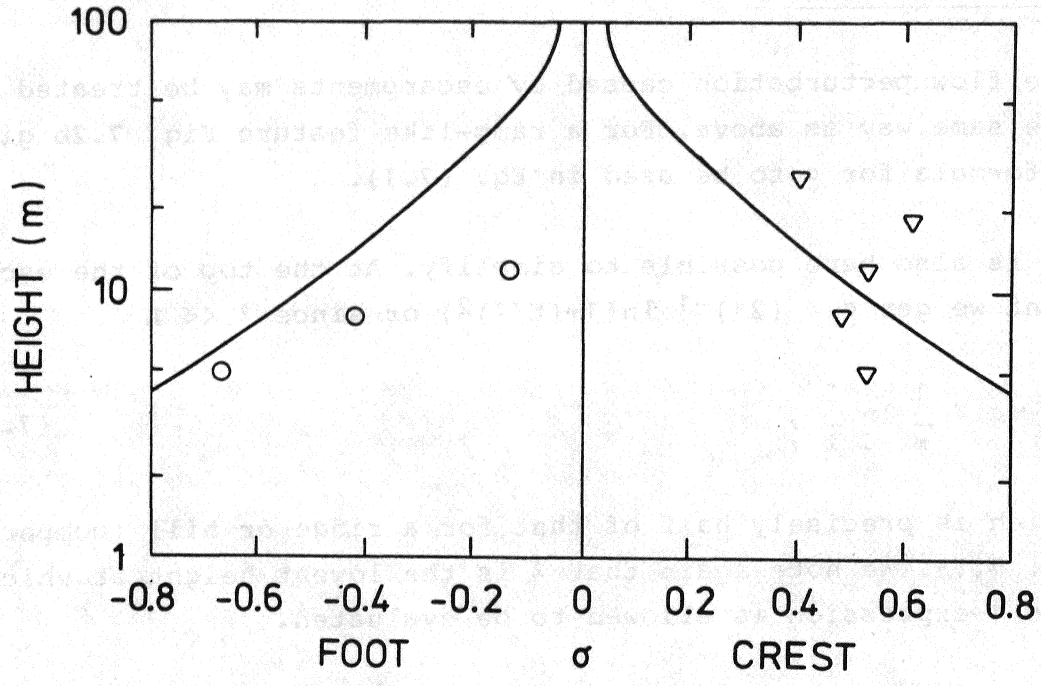

Fig. 7.3. Comparison of the parameter σ calculated from experimental data and from the expression given in Fig. 7.2b for a ramp-like escarpment. Details of this comparison is given in Jensen (1983).

which, as pointed out by Jensen and Peterson (1978), has the consequence that x replaces L in Eq. (7.9) in determining the effective "slope" of the terrain whereby downwind of an escarpment

$$\Delta s \propto \frac{h}{x} \qquad (7.12)$$

irrespective of the shape of the escarpment. Compared with scanty full scale data and some wind tunnel measurements (e.g. Bowen and Lindley, 1977), the decay of Δs with distance according to (7.12) is much too fast.

In another way the actual slope of the ramp loses importance. The above results are only valid for quite gentle slopes. For steep slopes the speed-up ceases to depend on h/L or the ramp

slope, because of separation. Thus Bowen and Lindley (1977) in a wind tunnel investigation using h/L = ∞, 1, 1/2, 1/4, got, in all four cases, a maximum fractional speed-up factor (above the crest) of about 0.7. This might be explained by the presence of an effective minimum slope introduced by the separation stream line on the windward side of the crest.

7.3. General

Further experimental data are needed to enable a good understanding of especially the later stages of the escarpment flow problem in the far downwind field. In addition it is required to get some information on the possible significant effect of atmospheric stability, some experiments are underway, but it is yet too early to report on them. It not yet possible to give general rules to cover these circumstances. Anyway using the above h/x rule it might be assumed that terrain effects are relatively unimportant at distances of 10 terrain heights away from the crest or summit. As explained above the overspeed resulting from an escarpment might be a bit more persistent. In vicinity of the summit quite reasonable estimates using the above formulae are possible. The vertical extend of the affected region is of order L which means that if the positive effect of a hill on available wind power is going to be used the hill must be of a sufficient length, i.e. many times longer than the hub height of the wind turbine.

8. CORRECTIONS FOR LOCAL SHELTER

Before any measured wind speed or frequency distribution can be utilized it is mandatory that some consideration is done as to possible local obstructions near the anemometer. This is not usually a major concern in the context of weather prediction or general climatology but becomes important in connection with

wind power. The WMO requirements to the anemometer location are not sufficient in order that the anemometer data are representative except very near the anemometer.

In order to correct the data for the effect of local sheltering an objective method based on the gustiness of the wind at the anemometer site can be employed. The method consists of two steps (Wieringa, 1976, 1977):

1) From the wind record the maximum gusts are extracted together with the corresponding mean wind speed. This is done for each azimuth wind direction sector during periods with strong wind (> 6 ms^{-1}). From these data an "effective" roughness length is derived.

2) Assuming the wind profile to be logarithmic up to a height z_b, above which the local sheltering effects vanish, the wind speed can be corrected using the transformation

$$u_r = u_s \frac{\ln(z_b/z_{os}) \cdot \ln(z_a/z_{or})}{\ln(z_a/z_{os}) \cdot \ln(z_b/z_{or})} \qquad (8.1)$$

where

u_s = observed wind speed
z_a = anemometer height usually 10 m
z_{os} = "effective roughness length" from gustiness analysis"
z_b = "roughness blending height" = 60 m
z_{or} = roughness length corresponding to unsheltered location = 0.03 m.

The method can be applied in cases where the necessary information regarding anemometer response is available either directly or can be derived by calibrating the instrumental constants in the gustiness analysis in one azimuth sector, where the terrain is so open and homogeneous that the roughness length can be estimated (see Section 5). This calibration, (Wieringa, 1982) is often preferable even if instrumental data are available since they are often unreliable in practice.

The sheltering effect of nearby single well definable objects such as large buildings or rows of trees has been investigated in a number of studies (Wegley et al., 1980; WMO tech note 59, 1964). For anemometer locations in the immediate wake (distance/object height < 5 and anemometer height $\tilde{<}$ object height) the influence is large and critically dependent on the geometry of the obstacle, and wind data difficult to correct. If the wind has to pass such large obstructions with a high frequency of occurrence (say > 25%) then it may be preferable not to use the data if possible.

For moderate sheltering the data can be corrected to unsheltered conditions using the empirical relations presented by Perera (1981):

$$S = \frac{\Delta u}{u} = 9.8 \left(\frac{z_a}{h}\right)^{0.14} \frac{x}{h} (1-p)\, \eta \exp(-0.67\, \eta^{1.5}) \qquad (8.2)$$

with

$$\eta = \frac{z_a}{h} \left(\frac{0.32}{\ln h/z_o} \cdot \frac{x}{h} \right)^{-0.47}$$

and

p = porosity = open area/total area
z_o = upstream surface roughness
h = height of obstacle
z_a = height of anemometer
x = distance downstream.

For nonporous obstacles and typical upwind conditions this result is shown in Fig. 8.1. The effect of porosity is accounted for approximately by multiplication of (1-p). Another consideration relevant for correction of wind data is the lateral dimensions of the obstacles. Most empirical data including the data in Perera (1981) are concerned with two dimensional fences or shelter belts corresponding to "infinite" lateral dimensions. The shelter from obstacles with finite lateral dimensions are

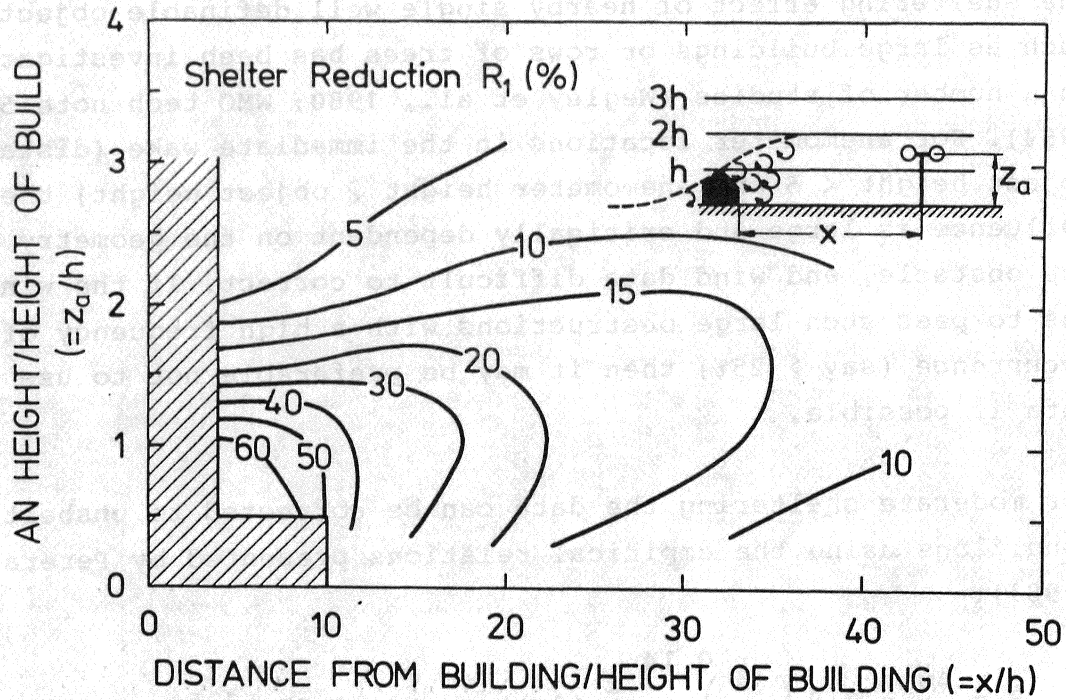

Fig. 8.1. Shelter reduction by two-dimensional obstacle. Based on the expressions given by Perera (1981).

decreased because of lateral mixing in the wake; and furthermore the effect on the average wind speed in a given azimuth sector is decreased because of the finite angular dimension of the obstacle as seen from the anemometer. The reduction in average wind speed in a given sector can be estimated approximately by reducing the shelter from Fig. 8.1 using the following expression derived from simple geometrical considerations:

$$R = \begin{cases} \left(1 + 0.2\,\frac{x}{L}\right)^{-1} & \text{for } \frac{L}{x} > \Delta\phi - 0.2 \\ \left(\frac{x}{L}\,\Delta\phi\right)^{-1} & \text{for } \frac{L}{x} < \Delta\phi - 0.2 \end{cases} \qquad (8.3)$$

where L is the lateral dimension of the obstacle and $\Delta\phi$ is the width of the azimuth sector. A similar correction procedure was employed in Petersen et al. (1981). Both shelter correction methods are based on conditions of neutral stability and anemometer location outside the immediate wake. In connection with

wind power applications this is not a problem, and correction of a frequency distribution can be done simply by rescaling the wind speed. For the Weibull distribution this corresponds to rescaling the A-parameter:

$$A_{cor} = A_{obs} \cdot (1-R \cdot S)^{-1} \qquad (8.4)$$

where A_{cor} is the A-parameter corresponding to unsheltered conditions, and A_{obs} the observed A-parameter.

9. HORIZONTAL EXTRAPOLATION

The problems of horizontal and vertical extrapolation or interpolation of wind data are closely related. In both cases the basic difficulties are related to inhomogeneities in the surface conditions. In this chapter we shall discuss the problems in connection with horizontal extrapolation of wind data over terrain where large orographic effects or frequent mesoscale forcing are not important. Even for this relatively simple type of conditions wind data obtained at low heights are typically representative only within a few hundred metres from the anemometer because of nearby changes in surface roughness. Other reasons for the unrepresentativeness can be the effect of hills and escarpments near the anemometer or even smaller scale perturbations due to nearby buildings etc.

The theory discussed in Chapters 6 to 8 enables a correction of this type of data to conditions over a hypothetical nearby open flat field. However, due to the fact that this theory is based on surface layer conditions the data can generally only be made representative to an area within a few kilometres. As an example consider the correction based on gustiness analysis (Chapter 8); an important assumption here is that a "roughness blending height" of 60 m exists where the wind speed is independent of the "local" surface conditions. From the discussion in Chapter 6

it follows that "local" in this case is within 1-2 km. The response of the wind profile to changes in surface conditions is not very well established beyond fetches larger than ~1 km. An attempt to extrapolate surface layer theories to larger fetches was presented by Larsen et al. (1981) and Hedegaard and Larsen (1983). Very little data exists, however, to test such extrapolations. Jensen (1978) shows that straight forward extrapolation of surface layer theory leads to a limiting behaviour of the boundary layer wind profile which is not consistent with the geostrophic drag-laws (Chapter 5), however, numerical results by Taylor (1969) and others suggest that the boundary layer reaches equilibrium of the order of 20 km downstream of a change in surface roughness under conditions of neutral stability. The results for simple roughness changes at short fetches make one thing apparent, namely that the downstream change of the wind speed at low heights happens most rapidly within the first 1-2 km with a subsequent very slow adjustment to equilibrium over the next 10-30 km. From these considerations it becomes clear that:

1) Straight-forward interpolation of mean wind speed between synoptic stations, to obtain iso-tach maps is not meaningful.

2) Even after careful screening and correction for local sheltering etc., interpolation is not meaningful in general, due to the separation of synoptic stations, which is typically not less than 50 km.

The problems with interpolation of mean wind speed is obviously also present with more sophisticated techniques based on the correlation matrix of wind data from a network of synoptic stations. The synoptic network is thus inadequate in terms of density when one wishes to map local wind conditions; however, it is in many parts of the world more than adequate in terms of resolving the overlying synoptic scale wind systems which force the wind in the boundary layer. With sufficient density of stations it is possible then to map the wind speed distributions for idealized conditions using only selected stations with min-

imal exposure problems. Such an approach is presently being taken in the wind energy programme in the European Economic Community (Petersen et al., 1982). The steps in the method are illustrated in Fig. 9.1. Initially a number of stations are selected which have minimal problems in terms of exposure, and where long time series (> 10 years) of meteorological parameters can be obtained. For the stations very accurate descriptions of anemometer location (and possible relocation) and surroundings are obtained preferably by site visits, and from these the surface roughness length is estimated for each azimuth sector, together with possible local sheltering. Using the theory described in the previous chapters with the schemes for the indirect estimation of surface heat flux (Holtslag and van Ulden, 1982, 1983) an estimate of the geostrophic wind is obtained. The geostrophic wind and the static stability over land can then be considered essentially constant over a few hundred kilometres enabling a meaningful interpolation between stations, or alter-

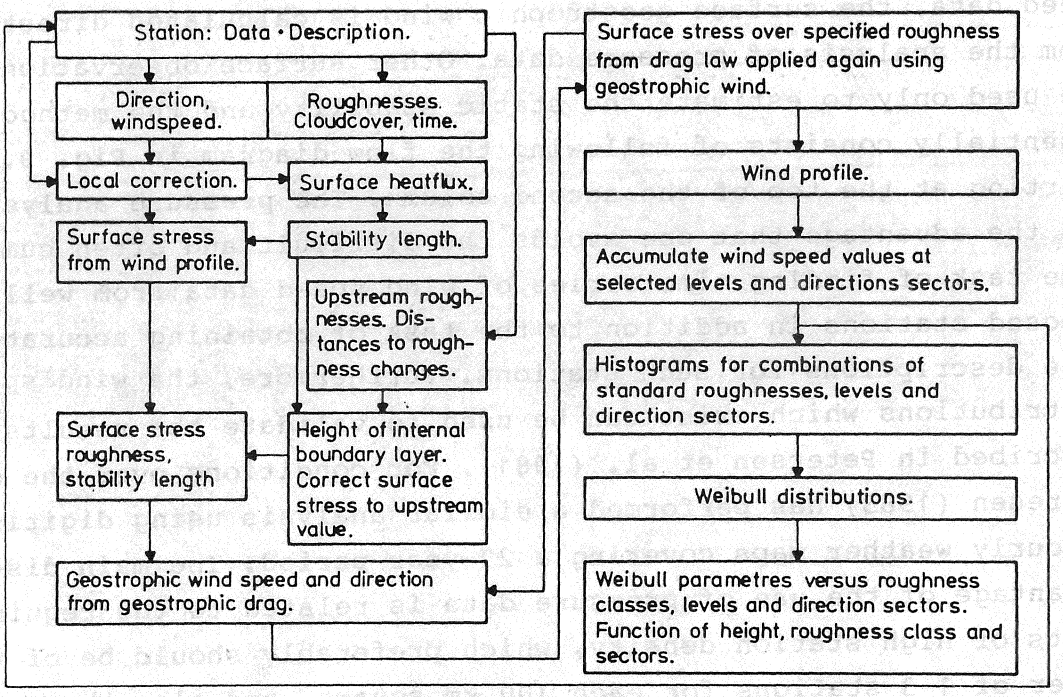

Fig. 9.1. Schematical representation of the computational scheme for the wind atlas for the EEC countries.

natively one single station can suffice and provide an estimate over an area of typically this dimension. The interpolated geostrophic wind can then be used for the inverse calculation, using the same theory, but calculating the wind speed and direction over a terrain with a specified surface rughness and possibly at another height (10-100 m). Performing this calculation for each 3 hourly observation over the 10-year period analysing the results in terms of the Weibull parameters A and k for each of 8 azimuth sectors, 4 types of terrain roughness and 4 heights (10, 25, 50 and 100 m) a description of wind conditions over idealized homogeneous flat terrain is obtained.

The manner with which these data can be used for the estimation of wind speed distribution, wind power "potential" at real sites is described in detail in Petersen et al. (1981).

In that publication a variation of the method described above was used to obtain the Weibull parameters over idealized terrain in Denmark. Instead of taking the starting point in real wind speed data, the surface geostrophic wind is calculated directly from the analysis of pressure data. Other surface observations are used only to estimate the static stability and the method essentially consists of following the flow diagram in Fig. 9.1 starting at the top of the second column. The pressure analysis has the advantage that one avoids the difficult and often cumbersome task of finding time series of wind speed data from well-exposed stations in addition to the task of obtaining accurate site descriptions for such stations. Furthermore, the wind speed distributions which exist can be used to validate the results as described in Petersen et al. (1981). For conditions over the sea Børresen (1983) has performed a similar analysis using digitized 6 hourly weather maps covering a 27-year period. The main disadvantage of the use of pressure data is related to the requirements of high station density, which preferably should be of the order of 1-3 stations for each 100 km square, and also there should be only small height differences between station in order that the reduction to sea level does not introduce to large spurious pressure gradients. As another alternative one could use wind data from radiosondes taking the wind speed at a pressure

level at approximately 2 km above the surface (850 mb over low lying terrain) and using this for the geostrophic wind, again applying the model described above. The three different methods described here all rely on the boundary layer theory discussed in Chapters 5 and 6 and can loosely be described as a double vertical extrapolation of the wind speed in the boundary layer starting with surface observations extrapolating to the top of the boundary layer, then interpolating or extrapolating the "free" wind in the horizontal and finally extrapolating to a specified height and surface conditions at a specified site. It is tempting to try to simplify this double transformation by using a logarithmic profile with or without a stability correction and extrapolating to a fixed height above terrain; however, there is little or no theoretical justification for such a procedure.

The loss of correlation in the wind field as determined by purely statistical methods applied to the synoptic network can to a large extent be explained by the theory described above. Thus the above methology or similar transformations of the raw data based on physical principles should always be applied before any statistical treatment.

The three methods based on the geostrophic drag law differ as noted above with respect to data requirements, also they differ with respect to the assumptions necessary for their theoretical justification. We shall not go into a discussion of these problems here, but note that presently it is not known which method is preferable in terms of practical applications. The methods all require the use of a computer. It is possible, as shown in the example below, to simplify the calculations in the case where radiosonde data are used, when we have to do with windy climates where conditions of neutral stability can be assumed.

Example 9.1

Figure 9.2 shows the iso-tach of the mean 850 mb wind analysed from weather maps over the North sea and from radiosondes over

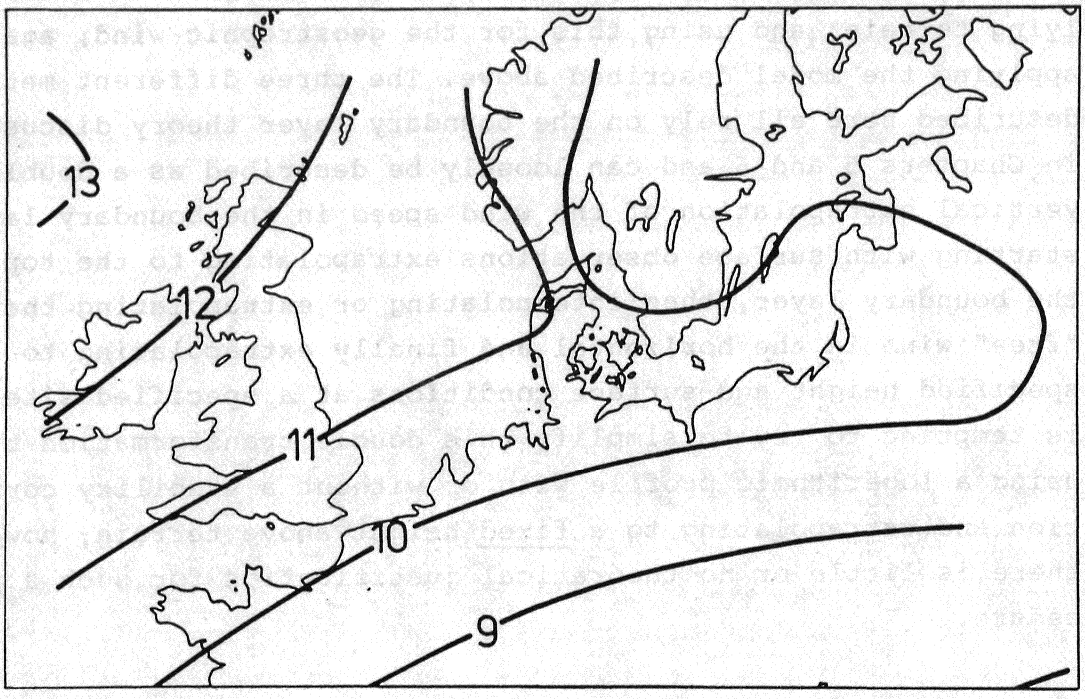

Fig. 9.2. The average height wind at 850 mb from analysis of weather maps and radiosonde data over Northern Europe.

central Europe. Taking as an example at a point in Denmark we can find a mean wind speed of 10.5 ms^{-1}. In Chapter 5 the following form of the geostrophic drag law is presented

$$\frac{u_*}{G} = \frac{0.5}{\ell n \left(\frac{G}{f z_o}\right)} \qquad (9.1)$$

Using G = 10.5 ms^{-1}, the appropriate Coriolis parameter f = $1.2 \cdot 10^{-4} s^{-1}$ and assuming a terrain with low surface roughness over land z_o = 0.01 m, we obtain u_* = 0.328 ms^{-1}; the logarithmic profile reads

$$u(z) = \frac{u_*}{k} \ln(z/z_o) \; ; \qquad (9.2)$$

using z = 10 m we obtain u(10) = 5.7 ms^{-1}.

This is then the expected mean wind speed over the most open type of terrain over land. The value is very close to the value of 5.6 ms^{-1} found in the more elaborate analysis in Petersen et al. (1981) and also to actual observed mean wind speeds over this type-of terrain. Using z_o = 0.0001-0.001 m appropriate for over sea conditions we obtain u(10) = 7.3-6.6 ms^{-1} with observed mean values over the sea close to 7 ms^{-1}.

The method can be elaborated by subdividing into azimuth sectors and treating each sector individually. This enables the estimation of mean wind speeds at for example coastal sites, which are most often interesting in connection with wind power.

The geostrophic wind in Denmark has the following mean values and frequency of occurrence in the eight sectors centered on the directions N, NE, E etc.

Table 9.1. Distribution of mean geostrophic wind speed in Denmark.

	N	NE	E	SE	S	SW	W	NW
mean ms^{-1}	8.1	7.8	9.1	9.8	10.4	11.4	11.6	10.7
freq. %	7.4	7.3	11.4	14.0	13.0	15.5	18.1	13.1

Using Eqs. (9.1) and (9.2) for each sector with a roughness distribution appropriate for a site at a westward facing coast and a height above terrain of 45 m we obtain the following table.

Table 9.2. Average wind speed computed for z = 45 m. The roughness length in the N and S sectors are taken as the logarithmic average of the land roughness of 5 cm and sea roughness of 0.3 mm because the coastline cuts through the middle of these sectors, also the sea roughness is taken as the geometrical average of 1 and 0.1 mm.

	N	NE	E	SE	S	SW	W	NW
z_o (m)	0.004	0.05	0.05	0.05	0.004	0.0003	0.0003	0.0003
mean speed (ms^{-1})	5.7	4.7	5.4	5.8	7.2	8.7	8.8	8.2

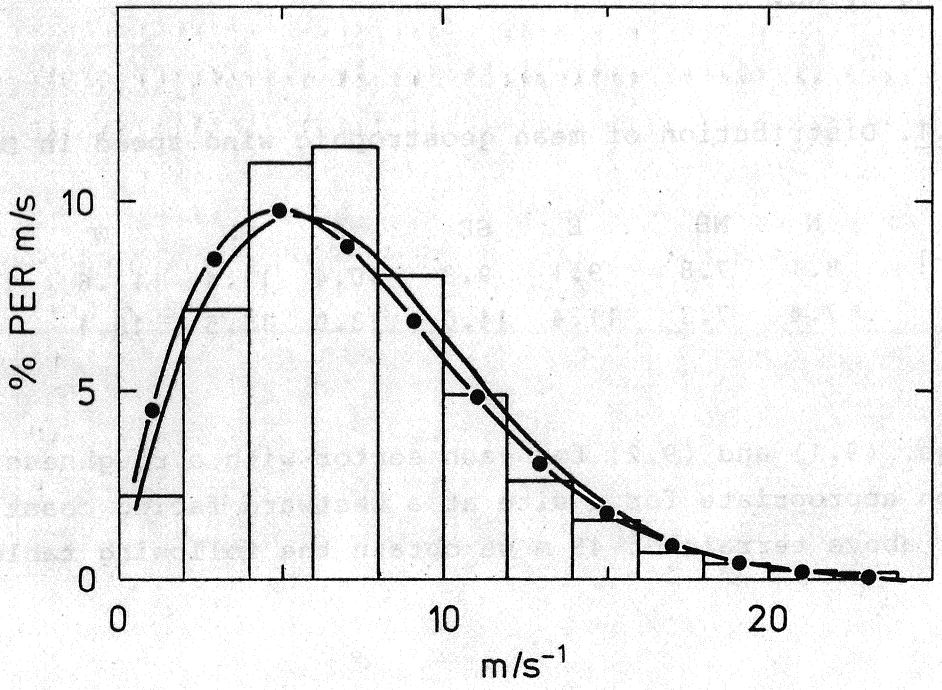

Fig. 9.3. Relative frequency of occurrence, measured and calculated, of wind speeds at the Nibe site at the height of 45 m.
Histogram: measured distribution.
——— : model by Petersen et al. (1981).
●——● : present simple estimate.

The average then becomes 7.2 ms^{-1}. Assuming the k-parameter in the corresponding Weibull distribution (Chapter 4) being equal to the k-parameter in the Weibull distribution for the geostrophic wind speed: k = 1.75. For most surface conditions this is a slight underestimation, but the error on the distribution is not significant. The Weibull parameters for the wind speed distribution becomes: A = 8.1, k = 1.75. The distribution is plotted in Fig. 9.3 together with the distribution obtained from the more elaborate treatment, and the observed distribution at the Nibe site in Denmark.

10. FLOW IN COMPLICATED TERRAIN

The term complicated or complex terrain is most often associated with terrain where orography plays an important role for the flow. The simplest type of orographic influence: flow over a single well definable hill has already been treated in Chapter 7. When the horizontal scale of the hill is of the order of 1 km or less the perturbation introduced by the hill can be treated with simple analytical theory at least for the prediction of the mean wind profile when the hill has a smooth slope. As the scale of the hill increases it becomes more difficult to treat the flow in terms of a perturbation superimposed on an "external" equilibrium flow. Hills and mountains with horizontal scales larger than 10 km give typically rise to pressure perturbations which can extend to the middle or upper troposphere; the boundary depth and structure can be strongly perturbed causing hydraulic intensification of the leeside flow as an example. In addition complicated local wind systems can be generated by diurnal and spatial variation of the surface heating on the slopes ("mountain and valley winds"). Many of these flow systems are described in Smith (1979) and more qualitatively in Hiester and Pennell (1981).

Terrain forms

The following classification of terrain types relevant for mapping of wind power potential was adopted for the EEC countries (Petersen, 1982). Originally it was devised by R.B. Smith. Refer to Smith (1979) for the theory of mountain flows.

1. Non-mountainous regions far away from mountains. Complications occur in the form of surface roughness inhomogeneities and sheltering effects. The theory of geostrophic drag law is applicable.

2. As the regions above (1) but with the additional complication of small scale smooth hills and valleys. Typical horizontal dimensions are less than 1 km. The flow can be treated as under (1) and the modifications introduced by the obstacles can be treated as in Jackson and Hunt (1975) (potential flow with modification from turbulence and wind shear).

3. Larger scale hills and valleys. Horizontal dimensions larger than 1 km. On these scales buoyancy effects are almost always important and under stable stratifications mountain waves are often present.

4. High mountain massifs disected by deep valleys. Depending on the local geometry of a peak, the winds at the peak may somewhat modified be representative of free atmosphere values. In the valleys the wind climate is dominated by thermally induced mountain valley winds. Except for leeside foehn the winds are decoupled from free atmosphere winds.

5. Broad sloping foreland regions. These regions are characterized by some distinct mechanisms caused by processes like channelling, deflection, leeside descent and low level jet. These mechanisms are often well known like:

   - Foehn (leeside descent caused by up-stream blocking and large scale mountain waves).

- Bize (blocking and deflection of low-level cold air).

- Bora (hydraulic intensification of cold air flow and channelling).

- Mistral and Tremontane (combined channelling, leeside descent and hydraulic intensification).

- Morning jet (low-level jet generated thermally by sloping terrain).

In other parts of the world this classification probably also applies. Local wind systems similar to the ones named under point 5 exists in other parts of the world but under different names.

In connection with wind power applications a number of special flows are not interesting simply because the wind speed is low. This includes typical mountain-valley winds driven by surface heating and in many cases slope slows caused by cold air drainage due to nighttime surface cooling.

Many different types of models have neen proposed for the description of flow over complicated topography, a review of the models in the most recent publications are presented in Walmsley (1983).

Models based on the full hydrodynamical equations and which include realistic physical parameterizations are necessary in order to handle the full spectrum of the flow types mentioned under pts. 4 and 5.

These models are presently basically research tools requiring large investments in terms of manpower and computer time. Even when such investments can be made the models require large amounts of input data which often are not available and as a result initialization procedures including educated guesses

often have to be used and the results may be critically dependent on this. The use of models of this type can be advisable in cases where specific questions are asked regarding flow structure for flows where the basic dynamical mechanisms and scales are known enabling the choice of appropriate model and possibly also enabling an evaluation of uncertainties or deficiencies of the model output. From the point of climatology this type of investigation can be useful for vertical and horizontal extrapolation of wind speed under specific conditions. If the wind climate in a region at moderate and high wind speeds are dominated by such flows the use of numerical simulations can be very valuable for the interpretation and extrapolation of climatic data. The numerical model most appropriate depends on the characteristic scales of the flow and references can be made to the review by Walmsley (1983).

Many efforts in particular initiated by the interest in modelling the transport of pollutants in complex terrain have concentrated on diagnostic models to obtain the three-dimensional wind field from available surface and/or upper air data. The simplest type of these models are usually termed "mass consistent models" because they produce a three-dimensional wind field which obey the equation of mass conservation. Since obviously no unique solution exists these models give different results. The most crucial step in the models are the construction from the point data of an initial guess field which then is adjusted to satisfy the continuity equation. With insufficient initial data coverage the guess field may be far from the real wind field and lead to large errors in the final result. Applied with care they can, however, provide some guidance for the estimation of wind structure in cases where the major effect of the orography is blocking and channelling of the flow. If thermal effects are important then these models require that sufficient data coverage resolve the flow, and furthermore it is not clear that introduction of mass conservation in the wind field analysis is warranted in such cases.

The two main advantages of the mass consistent models are low requirements to computer time and the linearity of the results.

The linearity is a result of the linearity of the continuity equation and means that the wind distribution at all points can be generated as a linear superposition of the results for a number of eigenvectors of the wind observations (Endlich et al., 1980). For the simplest case where only one set of data is used as input (f.ex. from one radiosonde) this means that only one model run has to be performed for each wind direction sector; for each sector model winds are proportional independent of the input wind speed.

In connection with vertical extrapolation of surface wind data only, extreme care must be taken when interpreting results from these simple models because of the arbitrary way the vertical wind profile is constructed in the initial guess field.

Vertical extrapolation of wind speed in generally complicated terrain where the flow is strongly ageostrophic needs, however, not necessarily present particular difficulties when the extrapolation is over moderate intervals, say between 10 m and 50 or 100 m even. Keeping in mind the relations presented in Chapter 7, namely the relation (valid for $x > L$):

$$\frac{\Delta u}{u} \sim \frac{h}{x} \qquad (10.1)$$

where $\Delta u/u$ is the relative velocity perturbation due to a hill, h is the height of the hill and x the downstream distance to the anemometer site. That is 20 or 30 heights downstream the perturbation is negligible. In "rough" terrain there may be no point this far away from the nearest terrain feature.

Equation (10.1) only applies for small hills with characteristic length $L < 1$ km; and for larger scale orographic features, we noted above that the situation is complicated by stratification effects (gravity waves) which can complicate the situation severely for the flow on the mountain slopes and near (that is $x \sim L$). For $x > L$, however, we must expect that the effect of the mountain in terms of the perturbation of the wind profile must be negligible also in this case.

The pressure perturbation caused by mountains with horizontal scales $L \gtrsim 10$ km extends to height above the boundary layer. In many cases it is not a simple task to determine an appropriate L to characterize the horizontal dimensions of terrain features. In some cases, however, a scale gap exists so that the terrain around the anemometer is homogeneous on a small scale, except possibly for local well definable features which can be handled by the theory in Chapter 7, even though the anemometer is located in the middle of a large mountainous region and the data strongly influenced by this climatically. In such cases the theory for the wind profile under homogeneous conditions also applies, in particular it is reasonable to use the simple profile expressions from Chapter 5 to vertical extrapolation over moderate height intervals.

In general the strongest perturbations of the wind profile are caused by the very local features, and it is more important to take these into account as accurately as possible following Chapter 7, when making vertical extrapolations, than attempting an analysis of the more complicated larger scale flow. The condition $x > L$ can be fulfilled as an example in the terrain form listed under point 5 in the classification above. This includes typically wide valleys between mountain massifs in which horizontal homogeneity exists on a small scale whereas the larger scale flow is strongly disturbed; as an example one may consider the mistral in the Rhône valley in France. This flow system which gives rise to high steady wind speeds is caused by complicated dynamical interplay of channelling, leeside descent and hydraulic intensification of flow between the Massif-Central and the Alps. In the lower part of the Rhône valley, however, the terrain is gently sloping over scales of the order of 50-100 km and we must expect the wind profile to be close to the logarithmic (plus stability corrections) up to heights comparable to the top of the surface boundary layer apart from perturbations due to smaller scale terrain features as described in Chapters 6, 7 and 8.

11. WIND MEASUREMENTS, OBSERVATIONS AND WIND STATISTICS

The average energy production of a given turbine at a given place can be calculated if the power curve of the wind turbine and the probability density function for the wind speed at hub height are known (cf. Chapter 3). Hence a 30-year series (which is the climatological standard) of reliably measured 10 minutes averaged wind speeds (cf. Chapter 2) would constitute the near optimal statistics for calculating the mean energy production for a given site at a given height. In a number of cases, the relevant wind statistics may be obtained by extrapolation as described above, but actual measurements at hub height may be the only means by which energy production from wind turbines placed in real rugged terrain can be estimated with a reasonable accuracy.

Having either acquired or determined to perform wind measurements at hub height the question arise to the necessary length of the time series. Generally it can be said that at least a year should be obtained in order to cover the yearly cycle and if possible three years or more due to the persistence in year to year's weather. Time series of a few months length can only be used with any reason if they can be linked (correlated) with a nearby longer measurement series. However, in this case a horizontal extrapolation is being performed and this has to follow the guidelines discussed in Chapter 9.

In Fig. 11.1 is shown the standard deviation relative to the mean production for various time intervals as calculated for a 45 m high wind turbine in Denmark over 21 years. Although the curve is site and height specific it shows the general feature that the variance or estimation error is decreasing with an increasing time interval. It is seen that the standard deviation is 30% of the mean value for 2 or 3 months production and 12% for the yearly production.

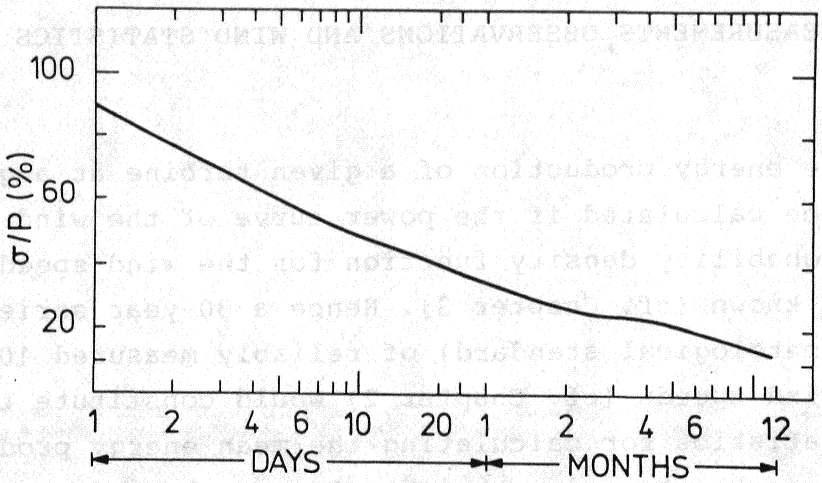

Fig. 11.1. The standard deviation (σ) of the power averaged over the period T relative to the mean power (P), (Petersen et al. 1981).

Observations

If measurements are performed at the site but not at hub height a vertical extrapolation has to be performed as described in the bulk of this report. Quite commonly, however, available wind speed statistics are not obtained by means of measurements but rather visual observations following the Beaufort scale. (Table 11.1). The analysis of such wind records is difficult and the uncertainty on the results often large. This is so for several reasons: The wind is estimated subjectively by an observer rather than being objectively measured by instruments; Observers and sites of observations may have changed over the time; The scale in which the winds are reported may have changed (in Denmark it changed from a seven-category land scale to the 13-category Beaufort scale in 1911, (Peterson, 1983)); the assignment of a numerical value to the observed wind is a subjective judgement and has no one-to-one correspondence with the actual wind speed (Alcock and Morgan, 1978). With these warnings it should be said that there are advantages in using the record of a trained observer who has recorded his observations using the Beaufort scale. Anemometer records are fallible; anemometers

Table 11.1. Beaufort's table for wind force and wind speed equivalence.

Beaufort number	Description	Velocity equivalent at a standard height of 10 metres above open flat ground			Specification for estimated speed over land	Specification for estimated speed over 'sea'
		Knots	Metres per second	Kilometres per hour		
0	Calm	<1	0-0.2	<1	Smoke rises Vertically	Sea like a mirror
1	Light air	1-3	0.3-1.5	1-5	Direction of wind shown by smoke-drift but not by wind vanes	Ripples with appearance of scales are formed, but without foam crests
2	Light breeze	4-6	1.6-3.3	6-11	Wind felt on face; leaves rustle; ordinary vanes moved by wind	Small wavelets, still short but more pronounced; crests have a glassy appearance and do not break
3	Gentle breeze	7-10	3.4-5.4	12-19	Leaves and small twigs in constant motion; wind extend light flag	Large wavelets; crests begin to break; foam of glassy appearance; perhaps scattered white horses
4	Moderate breeze	11-16	5.5-7.9	20-28	Raises dust and loose paper; small branches are moved	Small waves, becomming longer; fairly frequent white horses
5	Fresh breeze	17-21	8.0-10.7	29-38	Small trees in leaf begin to sway, crested wavelets form on inland water	Moderate waves, taking a more pronounced long form; many white horses are formed (chance of some spray)
6	Strong breeze	22-27	10.8-13.8	39-49	Large braches in motion; inconvenience felt when walking against the wind	Large waves begin to form; the white foam crests are more extensive everywhere (probably some spray)
7	Near gale	28-33	13.9-17.1	50-61	Whole trees in motion; inconvenience felt when walking against the wind	Sea heaps up and white foam from breaking waves begins to be blown in streaks along the direction of the wind
8	Gale	34-40	17.2-20.7	62-74	Breaks twigs off trees; generally impedes progress	Moderately high waves of greater length; cages of crests begin to break into the spindrift. The foam is blown in well marked streaks along the direction of the wind
9	Strong gale	41-47	20.8-24.4	75-88	Slight structural damage occurs (chimney-pots and slates removed)	High waves; dense streaks of foam along the direction of the wind; crests of waves begin to topple, tumble and roll over; spray may affect visibility
10	Storm	48-55	24.5-28.4	89-102	Seldom experienced inland; trees uprooted; considerable structural damage occurs	Very high waves with long overhanging crests; foam, in great patches, is blown in dense white streaks along the wind. On the whole the surface of the sea takes a white appearance; the tumbling of the sea becomes heavy and shocklike; visibility affected
11	Violent storm	56-63	28.5-32.6	103-117	Very rarely experienced; widespread damage	Exeptionally high waves; the sea is completely covered with long white by patches of foam lying in the direction of the wind; the edges of the waves are blown into froth; visibility affected
12	Hurricane	64 and over	32.7 and over	118 and over		The air is filled with foam and spray; sea completely white with driving spray; visibility very sereously affected.

are quite often poorly sited, so that their measurements are not representative of the overall wind conditions in the area; they do not always operate properly; their maintenance may not be sufficient; and for low wind speeds they may not operate at all.

A trained observer, on the other hand, can record overall wind conditions, can distinguish between calm and low wind speeds, and naturally tends to report an integrated observation of the prevailing conditions rather than making a nearly instantaneous observation of the present wind speed and direction at a particular location. The Beaufort system of wind classification can be a rather useful if imprecise measure of the state of the wind.

Sometimes visual observations are supplemented by measurements of the Daily Wind Run. The anemometer is then read of once a day giving in miles the distance travelled by the wind in the preceeding 24 hours. The conversion to metric units is

$$u(ms^{-1}) = 0.0185 \times \text{Daily Wind Run (miles)}$$

Table 11.2. Lodwar Meteorological Station, Kenya.

MONTH	DAILY WIND RUN (1967–70)	WIND SPEED (1946-70)		CALMS (1966–70)	
		0600 GMT	1200 GMT	0600 GMT	1200 GMT
	miles	knots	knots	days	days
January	100.8	5	12	7	1
February	107.8	5	13	6	0
March	117.0	6	13	2	1
April	121.5	7	11	2	0
May	113.1	8	10	1	1
June	112.1	9	9	1	0
July	122.2	9	9	1	1
August	123.1	9	10	1	1
September	131.0	10	10	1	0
October	138.9	9	12	0	0
November	137.7	7	12	2	1
December	107.7	4	12	6	1
Year	119.4	7	11	30	7

Table 11.2 is taken from Climatological Statistics for East Africa, East African Meteorological Department (1975). If the average diurnal variation of the wind speed is considered to be sinussoidal, which is often the case, with the 6 GMT observation representing the minimum and the 12 GMT the maximum,

then the average wind speed at 10 metres height could be estimated as 0.5(7 kt + 11 kt) = 4.5 ms^{-1}. Further the Daily Wind Run can be used to estimate the mean wind speed. It appears from the table that the yearly average at two metres is 119.4 miles/day corresponding to 2.2 ms^{-1}. The anemometer is (was) situated with surrounding low buildings and trees. An estimate of the roughness is then z_o = 0.4 m (see Fig. 5.1) and a logarithmic extrapolation to 10 metre gives 4.4 ms^{-1}. This is close to the estimated value from the visual observations. It should be noted that a logarithmic extrapolation requires average neutral conditions which cannot be expected for this station. The reason for the good agreement can beside pure coincidence be attributed to the fact that the neutral value at 10 metres is almost halfway between the stable value to be expected at 6 GMT and the unstable value at 12 GMT. An estimate of the wind speed statistics at 10 metre which can be obtained from Table 11.2 is then u = 4.5 ms^{-1}. With a guessed k = 2 we have A = 4.5/0.886 = 5 ms^{-1}.

Sometimes climatological tables in addition to the three wind speed columns in Table 11.2 also have number of gales > Be 8 (18 ms^{-1}, cf. Table 11.1). In principle this information can be used to determine k when A has been estimated, but with a very high uncertainty due to the infrequent occurrences of such extremes. If, however, the exceedance of a value closer to the mean was known say $Pr(u > u_E) = p$ then from Eq. 4.2 the following expression for k can be obtained

$$k = \frac{\ln(-\ln(p))}{\ln(u_E) - \ln(A)} \qquad (11.1)$$

For example, if it is known that u = 4 ms^{-1} and the frequency of exceeding u = 6 ms^{-1} is 15% then (with A = 4/0.87 = 4.5 ms^{-1})

$$k = \frac{\ln(-\ln(0.15))}{\ln(6) - \ln(4.5)} \cong 2.2$$

Measurements

Meteorological measurement programs which are carried out in connection with wind energy investigations usually have two main usages: The estimation of the wind energy resource available for a certain region and the estimation of the mean energy production from a specific wind turbine at a specific location. The latter usage is also connected with the search for the optimal site inside a certain area. Zambrano (1980), Hiester and Pennell (1981) and WMO-No. 175 describe and give practical examples on the use of a variety of methods ranging from usual instrumented meteorological masts to the use of biological and geomorphological indicators. The basic idea of using biological and geomorphological indicators is that persistent winds in a region can cause deformation of vegetation, especially trees and eolian landforms such as dunes. These methods are still in the early being and can at present not be considered as means for reliable wind potential estimates.

With respect to the problem of designing a measurement program for investigating the wind energy resource of a region (scale of a few hundred kilometres) a few important points should be emphasized:

When the region is of types 1, 2 and 5 (Chapter 10), rather than putting up a dense network of small meteorological masts it is much better to have but a few perfectly sited masts (no obstructions and with homogeneous surroundings) that can resolve the statistics of the overall wind field as explained in Chapter 9.

The higher the measuring heights the better, the meteorological standard of 10 metres is not relevant in this connection.

The reader's attention is directed to the previously mentioned Climate Application Referral System, Wind Energy (WCP-56, WMO 1983), and especially for the subject of this chapter, entries under key word: "Instruments, equipment and data handling".

12. BIBLIOGRAPHY

ALCOCK, R.K. and MORGAN, D.G. (1980). Investigations of wind and sea state with respect to the Beaufort scale. Weather 33, 271-277.

ARYA, S.P.S. (1975). Geostrophic drag and heat transfer relations for the atmospheric boundary layer. Quart. J. Roy. Met. Soc. 101, 147-161.

ARYA, S.P.S. (1977). Suggested revisions to certain boundary layer parameterization schemes used in atmospheric circulation models. Mon. Wea. Rev. 105, 215-227.

BARNDORFF-NIELSEN, O. (1977). Exponentially decreasing distributions for the logarithm of particle size. Proc. R. Soc. Lond. Ser. A 353, 401-419.

BLACKADAR, A.K., TENNEKES, H. (1968). Asymptotic similarity in neutral barotropic boundary layer. J. Atmos. Sci. 25, 1015-1020.

BOWEN, A.J. and LINDLEY, D. (1977). A wind tunnel investigation of the wind speed and turbulence characteristics close to the ground over various escarpment shapes. Boundary-Layer Meteor. 12, 259-271.

BRADLEY, E.F. (1983). The influence of thermal stability and angle of incidence on the aceleration of wind up a slope. Proceedings of the 6th Int. Conf. on Wind Eng., Auckland, New Zealand, April 6-7, 1983, Session 21.

BUSINGER, J.A. (1973). Turbulent transfer in the atmospheric surface layer. Workshop on Micrometeorology, D.A. Haugen, Ed., Amer. Meteor. Soc., 67-100.

BUSINGER, J.A., WYNGAARD, J.C., IZUMI, Y. and BRADLEY, E.F. (1971). Flux-profile relationships in the atmospheric surface layer. J. Atmos. Sci. 28, 181-189.

BUSINGER, J.A. and ARYA, S.P.S. (1974). The height of the mixed layer in the stably stratified planetary boundary layer. Advances in Geophysics, Vol. 18A. Academic Press, 73-92.

BØRRESEN, J.A. (1983). The Vector-Wind-Field at the Norwegian Continental Shelf. The Norwegian Meteorological Institute. Environmental Data Center.

CLARKE, R.H. (1970). Observational studies in the atmospheric boundary layer. Quart. J. Roy. Met. Soc. 96, 91-114.

CLARKE, R.H. and HESS, G.D. (1973). On the appropriate scaling for velocity and temperature in the planetary boundary layer. J. Atmos. Sci. 30, 1346-1353.

CLARKE, R.H. and HESS, G.D. (1974). Geostrophic departure and the functions A and B of Rossby-number similarity theory. Boundary-Layer Meteor. 7, 267-287.

DEARDORFF, J.W. (1970). Preliminary results from numerical integrations of the unstable planetary boundary layer. J. Atmos. Sci. 27, 1209-1211.

DEARDORFF, J.W. (1972). Parameterization of the planetary boundary layer for use in general circulation models. Mon. Wea. Rev. 100, 93-106.

DYER, A.J. and BRADLEY, E.F. (1982). An alternative analysis of flux-gradient relationships at the 1976 ITCE. Boundary-Layer Meteoro. 22, 3-19.

EAST AFRICAN METEOROLOGICAL DEPARTMENT (1975). Climatological statistics for East Africa. Part I, Kenya. 92 pp.

ELLISON, T.H. (1956). Atmospheric turbulence. Surveys in Mechanics, edited by G.K. BATCHELOR and R.M. DAVIS, Cambridge University Press, Cambridge, U.K. pp. 475.

ENDLICH, R.M., LUDWIG, F.L. and BHUMRALKAR, C.M. (1982). A Diagnostic Model for Estimating Winds at Potential sites for Wind Turbines. J. Appl. Meteor. 21, 1441-1454.

ESDU 72026 (1972). Characteristics of wind speed in the lowest layers of the atmosphere near the ground: Strong winds. Eng. Sci. Data Unit, Ltd., 251 Regent St., London WIR 7AD.

FRANDSEN, S. and CHRISTENSEN, C.J. (1980). On Wind Turbine Power Measurements. Proceedings of the 3rd Int. Symp. Wind Energy Syst. Aug. 28-29, 1980, Copenhagen, Denmark.

FRANDSEN, S., TRENKA, A.R. and PEDERSEN, B.M. (1982). Recommended Practices for wind turbine testing: 1. Power performance testing, IEA Executive Committee on R & D on WECS.

GOLDER, D. (1972). Relation among stability parameters in the surface layer. Boundary Layer Meteor. 3, 47-58.

HEDEGAARD, K. (1982). Wind vector and extreme wind statistics in Greenland. Danish Meteorological Institute. Weather Service Report No. 1, 106 pp.

HEDEGAARD, K. and LARSEN, S.E. (1983). Wind speed and direction changes due to terrain effects revealed by climatological data from two sites in Jutland. Risø-R-434, 120 pp.

HIESTER, T.R. and Pennell, W.T. (1981). The Siting Handbook for Large Wind Energy Systems. Pacific Northwest Laboratory. Richland, Washington 99352. Windbooks.

HOLTON, J.R., WALLACE, J.H. and YOUNG, J.A. (1971). On the Boundary Layer Dynamics and the ITCZ. J. Atm. Sci. 28, 275-280.

HOLTSLAG, A.A.M. and VAN ULDEN, A.P. (1982). Simple estimates of nighttime surface fluxes from routine weather data. Scientific report 82-4, Royal Netherlands Meteorological Institute, De Bilt, 15 pp.

HOLTSLAG, A.A.M. and VAN ULDEN, A.P. (1983). A simple scheme for daytime estimates of the surface fluxes from routine weather data. J.C. Appl. Meteor. 22, 517-529.

HÖGSTRÖM, U. (1974). A field study of the turbulent fluxes of heat, water vapour and momentum at a typical agricultural site. Quart. J. Roy. Met. Soc. 100, 624-639.

JACKSON, P.S. (1979). The influence of local terrain features on the site selection for wind energy generating systems. Faculty of Engineering Science, University of Western Ontario, Report BLWT-1-1979. pp. 83.

JACKSON, P.S. and HUNT, J.C.R. (1975). Turbulent wind flow over a low hill. Quart. J. Roy. Met. Soc. 101, 929-955.

JENSEN, N.O. (1978). Cahnge of surface roughness and the planetary boundary layer. Quart. J. Roy. Met. Soc. 104, 351.

JENSEN, N.O. (1981). Studies of the atmospheric surface layer during change in surface conditions. In: Colloque Construire avec le vent, CSTB, Nantes, France, June 15-19, 1981, Tome I No. I-4 (Centre Scientifique et Technique du Bâtiment, Nantes), 20 pp.

JENSEN, N.O. (1983). Escarpment induced flow perturbations, a comparison of measurements and theory. Proceedings of the 6th Int. Conf. on Wind Eng., Auckland, New Zealand, April 6-7, 1983, Session 21.

JENSEN, N.O. and PETERSON, E.W. (1978). On the escarpment wind profile. Q. J. Roy. Met. Soc. 104, 719-728.

KRISHNA, K. (1980). The planetary-boundary-layer model of Ellison (1956) - A retrospect. Boundary-Layer Meteor. 19, 293-301.

KRISTENSEN, L. and JENSEN, N.O. (1979). Lateral coherence in isotropic turbulence and in the natural wind. Boundary-Layer Meteor. 17, 353-373.

KRISTENSEN, L., PANOFSKY, H.A. and SMITH, S.D. (1981). Lateral coherence of longitudinal wind components in strong winds. Boundary-Layer Meteor. 21, 199-205.

LARSEN, S.E., HEDEGAARD, K. and TROEN, I. (1982). The change of terrain roughness problems extended to mesoscale fetches. In: Proc. from First International Conference on Meteorology and Air/Sea Interaction of the Coastal Zone, The Hague, Netherlands (Amer. Meteor. Soc., Boston, US. and KMNI, Netherlands), 8-13.

LETTAU, H.H. (1959). Wind profile, surface stress and geostrophic drag coefficients in the atmospheric surface layer. Adv. Geophys. 6, 241-257.

LETTAU, H.H., Davidson, B. (1957). Exploring the atmosphere's first mile. Pergamon Press, Vol. 1, 578 pp., Vol. 2, 376 pp.

LO, A.K. (1979). On the determination of boundary layer parameters using velocity profile as the sole information. Boundary-Layer Meteor. 17, 465-484.

LOUIS, J.-F. (1979). A parametric model of vertical eddy fluxes in the atmosphere. Boundary-Layer Meteor. 17, No. 2, 187-202.

LUMLEY, J. and PANOFSKY, H.A. (1964). The structure of atmospheric turbulence. Interscience-Wiley, New York, 239 pp.

LYNCH, R.A. and BRADLEY, E.F. (1974). Shearing Stress meter. J. Appl. Meteor. 13, 588-591.

MELGAREJO, J.W. and DEARDORFF, J.W. (1974). Stability functions for the boundary-layer resistance laws based upon observed boundary-layer heights. J. Atmos. Sci. 31, 1324-1333.

MONIN, A.S. and OBUKHOV, A.M. (1954). Basic regularity in turbulent mixing in the surface layer of the atmosphere. Trans. Geophys. Inst. Acad. Sci. USSR, No. 24 (151), 163-187.

PANOFSKY, H.A. (1973). Tower Micrometeorology Workshop on Micrometeorology, D.A. HAUGEN Ed., Amer. Meteor. Soc., 151-176.

PASQUILL, F. (1961). The estimation of the dispersion of windborne material. The Meteorol. Mag. 90, 33-49.

PASQUILL, F. (1972). Some aspects of boundary layer description. Quart. J. Roy. Met. Soc. 98, 417.

PERERA, M.D. (1981). Shelter behind two-dimensional solid and porous fences. J. of Wind Engin. and Industrial Aerodyn. 8, 1981, 93-104.

PETERSEN, E.L. (1982). Report from the action coordinator in: "Wind Energy", Proc. of the EC contractors meeting in Brussels, November 23-24 1982. Vol. 1, series G. Ed. W. PALZ and W. SCHNELL. D. Reidel Publishing Company. 220 pp.

PETERSEN, E.L., TROEN, J., FRANDSEN, S. and HEDEGAARD, K. (1981). Windatlas for Denmark. Risø-R-428, 229 p.

PETERSON, E.W. (1983). A study of the weather record from Fanø (1872-1980) including an analysis of climate variation. Risø-R-438, 70 p.

PETERSON, E.W., KRISTENSEN, L. and SU, C.C. (1976). Some observations and analysis of wind over nonuniform terrain. Quart. J. Roy. Met. Soc. 102, 857-869.

PETERSON, E.W., TAYLOR, P.A., HØJSTRUP, J., JENSEN, N.O., KRISTENSEN, L. and PETERSEN, E.L. (1980). Risø 1978: Further investigations into the effect of local terrain irregularities on tower-measured wind profiles. Boundary-Layer Meteor. 19, 303-313.

RIJKOORT, P.J. and WIERINGA, J. (1983). Extreme wind speeds by compound Weibull analysis of exposure-corrected data. Proceeding of the 6th International Conference on Wind Engineering, Australia, March 1983. 12 p.

SMITH, R.B. (1979). "The Influence of Mountains on the Atmosphere" in vol. 21 of Advances in Geophysics Ed. B. SALTZMANN Academic Press.

TAYLOR, P.A. (1969). The planetary boundary layer above a change in surface roughness. J. Atmos. Sci. 26, 432-440.

TAYLOR, P.A. and GENT, P.R. (1974). A model of atmospheric boundary layer flow above an isolated two-dimensional "hill"; an example of flow above "gentle topography". Boundary-Layer Meteor. 7, 349-362.

TAYLOR, P.A. and TEUNISSEN (1983). Progress report to the International Energy Agency's Programme of Research and Development on Wind Energy Conversion Systems, Task VI: Study of Local Wind Flow at Potential WECS Hill Sites. Atmospheric Environment Service, Canada.

VAN ULDEN, A.P. (1978). Simple estimates for vertical diffusion from a source near the ground. Atmos. Env. 12, 2124-2129.

WALMSLEY, J.L. (1983). Modelling the Boundary-Layer Wind Flow above Complex Terrain: A Review. Air Quality and Inter-Environment Research Branch Boundary Layer Research Division. Atmospheric Environment Service, 4905 Dufferin Street Downsview, Ontario, Canada M3H5T4 report AQRB-83-005-L.

WCP-56. Climate Application Referral System. Solar Energy-Wind Energy. WMO, Geneva, August 1983. 156 p.

WEGLEY, H.L., ORGIL, M.M., DRAKE, R.L. (1978) Siting Handbook for small Wind Energy Conversion Systems. Batelle, Pacific Northwest Laboratory, Richland Washington 99352 USA (PNL 2521).

WIERINGA, J. (1976). An objective exposure correction method for average wind speeds measured at a sheltered location. Quart. J. Roy. Met. Soc. 102, 241-253.

WIERINGA, J. (1977). Wind representativity increase due to an exposure correction obtainable from past analog station wind records. Proceedings of the WMO Technical Conference on Instruments and Methods of Observation, World Meteorological Organization, Geneva. No 480, 39-44.

WIERINGA, J. (1982). Description requirements for assessment of non-ideal wind stations - for example Aachen. Presented at the 5th colloquium on Industrial Aerodynamics, Aachen, June 1982.

WMO Commission for Atmospheric Sciences (1971). Observational requirements of lower tropospheric soundings. Boundary-Layer Meteor. 2, 127-129.

WMO tech. note No. 59 (1964). Windbreaks and shelterbelts. World Meteorological Organization, Geneva, Switzerland.

WMO tech. note No. 165 (1979). The planetary boundary layer (G.A. McBEAN, Ed.). World Meteorological Organization, Geneva, Switzerland.

WMO tech. note No. 175 (1981). Meteorological aspects of the utilization of wind as an energy source. World Meteorological Organization, Geneva, Switzerland.

WORLD SURVEY OF CLIMATOLOGY. Vol. 1-15. Editor: H.E. LANDSBERG. Elsevier.

WYNGAARD, J.C. (1975). Modelling the planetary boundary layer. Extension to the stable case. Boundary-Layer Meteor. 9, 441-460.

WYNGAARD, J.C., ARYA, S.P.S. and COTÉ, O.R. (1974). Some aspects of the structure of convective planetary boundary layers. J. Atmos. Sci. 31, 747-754.

ZAMBRANO, T.G. (1980). Assessing the local windfield with instrumentation. Pacific Northwest Laboratory, Richland, Washington 99352.

ZILITINKEVICH, S.S., LAIKHTMAN, D.L. and MONIN, A.S. (1967). Dynamics of the atmospheric boundary layer. Izv. Atmos. Ocean Phys. 3, 170-191 (English Edition).

ZILITINKEVICH, S.S., CHALIKOV, D.V. (1968). The laws of resistance and of heat and moisture exchange in the interaction between the atmosphere and an underlying surface. Izv. Atmos. Ocean Phys. 4, 438-441 (English Edition).

ZILITINKEVICH, S.S., DEARDORFF, J.W. (1974). Similarity theory for the planetary boundary layer of time dependent height. J. Atmos. Sci. 31, 1449-1452.

REPORTS PUBLISHED IN THE WORLD CLIMATE PROGRAMME SERIES

WCP - 1 INFORMAL PLANNING MEETING ON WORLD CLIMATE PROGRAMME (FOOD) (GENEVA, 10-14 NOVEMBER 1980)

WCP - 2 PRELIMINARY PLAN FOR THE WORLD CLIMATE RESEARCH PROGRAMME (GENEVA, JANUARY 1981)

WCP - 3 JOINT WMO/ICSU/UNEP MEETING OF EXPERTS ON THE ASSESSMENT OF THE ROLE OF CO_2 ON CLIMATE VARIATIONS AND THEIR IMPACT (VILLACH, AUSTRIA, NOVEMBER 1980)

WCP - 4 CONFERENCE STATEMENT AND PANEL REPORTS OF THE TECHNICAL CONFERENCE ON CLIMATE FOR ASIA AND THE WESTERN PACIFIC (GUANGZHOU, CHINA, 15-20 DECEMBER 1980) (out of print: has been incorporated into the Report of the Conference which has been published as WMO Publication No. 578)

WCP - 5 INFORMAL PLANNING MEETING ON WORLD CLIMATE PROGRAMME - WATER (GENEVA, 2-6 FEBRUARY 1981) (out of print)

WCP - 6 THE INTERNATIONAL SATELLITE CLOUD CLIMATOLOGY PROJECT (GENEVA, JANUARY 1981) (out of print)

WCP - 7 REPORT OF THE THIRD MEETING OF THE JSC WORKING GROUP ON HYDROLOGY AND LAND SURFACE PROCESSES (COLLEGE PARK, MARYLAND, USA, 10 JANUARY 1981) (out of print)

WCP - 8 REPORT OF THE MEETING ON THE COORDINATION OF PLANS FOR FUTURE SATELLITE OBSERVING SYSTEMS AND OCEAN EXPERIMENTS TO BE ORGANIZED WITHIN THE WCRP (CHILTON, U.K., 26-31 JANUARY 1981) (out of print)

WCP - 9 SUMMARY REPORT OF THE INFORMAL PLANNING MEETING ON THE WEST AFRICAN DATA BANK (GENEVA, 25-27 FEBRUARY 1981) (out of print)

WCP - 10 MEETING OF SELECTED EXPERTS ON CLIMATE-RELATED MONITORING (GENEVA, 21-24 APRIL 1981)

WCP - 11 JSC/CCCO MEETING ON TIME SERIES OF OCEAN MEASUREMENTS (TOKYO, 11-15 MAY 1981) (out of print)

WCP - 12 MEETING OF JSC EXPERTS ON AEROSOLS AND CLIMATE (GENEVA, 27-31 OCTOBER 1980)

WCP - 13 PLAN FOR WCP DEMONSTRATION PROJECTS - FOOD, ARISING FROM INFORMAL FAO/WMO MEETING OF EXPERTS (GENEVA, 27-31 JULY 1981)

WCP - 14 PAPERS PRESENTED AT THE WMO/ICSU/UNEP SCIENTIFIC CONFERENCE ON ANALYSIS AND INTERPRETATION OF ATMOSPHERIC CO_2 DATA (BERN, 14-18 SEPTEMBER 1981) (out of print)

WCP - 15 REPORT OF THE INFORMAL PLANNING MEETING ON WCP DATA REFERRAL SYSTEM (GENEVA, 28 SEPTEMBER - 2 OCTOBER 1981) (out of print)

WCP - 16 REPORT OF THE INFORMAL PLANNING MEETING ON WCP ENERGY (ROSKILDE, 1-3 DECEMBER 1981)

WCP - 17 REPORT OF THE WCP DATA MANAGEMENT MEETING (GENEVA, 16-20 NOVEMBER 1981) (out of print)

WCP - 18 EXTENDED CLOUDS AND RADIATION, BY C.M.R. PLATT, AUSTRALIA. A REPORT COMPILED FOR THE INTERNATIONAL RADIATION COMMISSION AND PRESENTED AT IAMAP (HAMBURG, AUGUST 1981)

WCP - 19 PLANNING GUIDANCE FOR THE WORLD CLIMATE DATA SYSTEM, BY R.L. JENNE (USA, FEBRUARY 1982)

WCP - 20 THE INTERNATIONAL SATELLITE CLOUD CLIMATOLOGY PROJECT (ISCCP) - PRELIMINARY IMPLEMENTATION PLAN (APRIL 1982)

WCP - 21 PAPERS PRESENTED AT THE JSC/CCCO MEETING ON TIME SERIES OF OCEAN MEASUREMENTS (TOKYO, 11-15 MAY 1981)

WCP - 22 REPORT OF THE JSC/CCCO "CAGE" EXPERIMENT: A FEASIBILITY STUDY (MAY 1982)

WCP - 23 REPORT OF THE SECOND INFORMAL PLANNING MEETING ON THE WEST AFRICAN DATA BANK (GENEVA, 19-23 APRIL 1982) (also available in French)

WCP - 24 FORMATS AND QUALITY CONTROL OF CLIMATOLOGICAL DATA FOR WEST AFRICA (out of print)

WCP - 25 OPTIMAL CLIMATE DATA UTILIZATION: A CLIMATIC DATA ACQUISITION, ARCHIVING, PROCESSING AND DISSEMINATION SYSTEM FOR RESOURCE MANAGEMENT. Prepared by Amos Eddy, Oklahoma Climatological Survey, September 1982.

WCP - 26 REPORT OF THE WMO/CAS-JSC-CCCO MEETING OF EXPERTS ON THE ROLE OF SEA ICE IN CLIMATIC VARIATIONS (GENEVA, 24-29 JUNE 1982) (out of print)

WCP - 27 REPORT OF THE PLANNING MEETING FOR THE MONSOON CLIMATE PROGRAMME (GENEVA, 28 JUNE - 1 JULY 1982)

WCP - 28 REPORT OF THE PLANNING MEETING ON INTERNATIONAL SATELLITE CLOUD CLIMATOLOGY PROJECT (ISCCP) (GENEVA, 9-12 AUGUST 1982)

WCP - 29 REPORT OF THE JSC/CAS MEETING OF EXPERTS ON DETECTION OF POSSIBLE CLIMATIC CHANGE, MOSCOW 3-6 OCTOBER 1982

WCP - 30 CLIMATE / ENERGY GRAPHICS: CLIMATE DATA APPLICATIONS IN ARCHITECTURE. By Vivian Loftness, Institute of Building Sciences in Carnegie-Mellon University, Pittsburgh, Pa, September 1982

WCP - 31 GUIDELINES ON CLIMATE DATA ORGANIZATION AND FORMATS (PREPARED BY THE INTER-COMMISSION MEETING ON CLIMATE DATA ARCHIVING FORMATS; GENEVA, 20-24 SEPTEMBER 1982) (also available in French and Spanish)

WCP - 32 FIRST CO-ORDINATION MEETING OF REGIONAL SOUTH EAST ASIAN CLIMATE DATA MANAGEMENT AND USER SERVICES (BANGKOK, 29 NOVEMBER - 3 DECEMBER 1982)

WCP - 33 BIBLIOGRAPHIE SUR LES REJETS DE CHALEUR/BIBLIOGRAPHY ON HEAT RELEASES Par/by D. Schneiter, Institut suisse de météorologie/ Swiss Meteorological Institute, janvier/January 1983

WCP - 34 CLOUD/RADIATION INTERACTION (SCIENTIFIC PAPERS PRESENTED AT JSC-III, DUBLIN, MARCH 1982)

WCP - 35 THE INTERNATIONAL SATELLITE CLOUD CLIMATOLOGY PROJECT (ISCCP) PRELIMINARY IMPLEMENTATION PLAN (REVISION 1, NOVEMBER 1982)

WCP - 36 SECOND PLANNING MEETING ON WORLD CLIMATE PROGRAMME - WATER (PARIS, NOVEMBER 1982)

WCP - 37 REPORT OF THE MEETING OF EXPERTS ON URBAN AND BUILDING CLIMATOLOGY (GENEVA, 6-10 DECEMBER 1982)

WCP - 38 REPORT OF THE WMO/ICSU STUDY CONFERENCE ON PHYSICAL BASIS FOR CLIMATE PREDICTION ON SEASONAL, ANNUAL AND DECADAL TIME SCALES (LENINGRAD, 13-17 SEPTEMBER 1982)

WCP - 39 BENEFICIAL USES OF CLIMATE. Prepared by Amos Eddy, Oklahoma Climatological Survey

WCP - 40 RADIATION BUDGET OF THE EARTH AND ITS ATMOSPHERE. By K. Ya. Kondratyev and E. Raschke with contributions from H.J. Preuss and J. Schmetz (out of print)

WCP - 41 THE EROSIVE CAPACITY OF RAINFALL. Roving Seminar paper by M.C. Babau (also available in French and Spanish)

WCP - 42 REPORT OF THE FIRST SESSION OF THE INTERNATIONAL WORKING GROUP ON DATA MANAGEMENT FOR THE INTERNATIONAL SATELLITE CLOUD CLIMATOLOGY PROJECT (ISCCP). (NEW YORK CITY, 13-17 DECEMBER 1982)

WCP - 43 TROPOSPHERIC AEROSOLS: REVIEW OF CURRENT DATA ON PHYSICAL AND OPTICAL PROPERTIES. Compiled by Franklin S. Harris, Jr., Scientific Editor, Hermann E. Gerber

WCP - 44 CLIMATE AND DESERTIFICATION: A revised analysis. By F. Kenneth Hare, Institute for Environmental Studies and Trinity College in the University of Toronto, Toronto, Canada, January 1983

WCP - 45 BIBLIOGRAPHY OF URBAN CLIMATE 1977-1980. Prepared by Professor T.R. Oke, Department of Geography, The University of British Columbia, Vancouver, B.C., Canada, June 1982

WCP - 46 REPORT OF THE JSC STUDY CONFERENCE ON LAND SURFACE PROCESSES IN ATMOSPHERIC GENERAL CIRCULATION MODELS, Greenbelt, Maryland, January 1981. Edited by P.S.Eagleson

WCP - 47 PHYSICAL BASIS FOR CLIMATE PREDICTION (Scientific Papers presented at Study Conference - Leningrad September 1982)

WCP - 48 REPORT OF THE MEETING OF EXPERTS ON THE FUTURE ACTIVITIES OF THE WORLD RADIATION CENTRE (WRC-LENINGRAD). (LENINGRAD, 28 FEBRUARY - 1 MARCH 1983)

WCP - 49 REPORT OF THE JSC/CCCO STUDY GROUP ON INTERANNUAL VARIABILITY OF THE TROPICAL OCEANS AND THE GLOBAL ATMOSPHERE (TOGA). (PRINCETON, 13-16 OCTOBER 1982)

WCP - 50 GUIDELINES ON CROP-WEATHER MODELS (WMO Task Force on Crop-Weather Models, 1983)

WCP - 51 PROPOSAL FOR THE PACIFIC TRANSPORT OF HEAT AND SALT (PATHS) PROGRAMME

WCP - 52 REPORT OF THE SECOND SESSION OF THE INTERNATIONAL WORKING GROUP ON DATA MANAGEMENT FOR THE INTERNATIONAL CLOUD CLIMATOLOGY PROJECT (ISCCP). (NEW YORK CITY, 25-27 MAY 1983)

WCP - 53 REPORT OF THE WMO (CAS) MEETING OF EXPERTS ON THE CO_2 CONCENTRATIONS FROM PRE-INDUSTRIAL TIMES TO I.G.Y. (BOULDER, USA, 22-25 JUNE 1983)

WCP - 54 VOLCANOES AND CLIMATE. By K. Ya. Kondratyev, (in preparation)

WCP - 55 REPORT OF WMO (CAS)/RADIATION COMMISSION OF IAMAP MEETING OF EXPERTS ON AEROSOLS AND THEIR CLIMATIC EFFECTS. (WILLIAMSBURG, VIRGINIA, USA, 28-30 MARCH 1983)

WCP - 56 CLIMATE APPLICATIONS REFERRAL SYSTEM. SOLAR ENERGY - WIND ENERGY. Geneva, August 1983

WCP - 57 PROCEEDINGS OF THE WORKSHOP ON CLIMATE DATA MANAGEMENT FOR THE AMERICAS. (BRASILIA, 11-15 APRIL 1983)

WCP - 58 REPORT OF THE MEETING WITH REPRESENTATIVES OF INTERNATIONAL ORGANIZATIONS ON WMO ACTIVITIES REGARDING URBAN AND BUILDING CLIMATOLOGY. (GENEVA, 14-15 JUNE 1983)

WCP - 59 PLAN FOR THE WORLD CLIMATE DATA PROGRAMME (AUGUST 1983) (also available in French, Spanish and Russian)

WCP - 60 REPORT OF THE FIRST SESSION OF THE JSC/CCCO WORKING GROUP ON SATELLITE OBSERVING SYSTEMS FOR CLIMATE RESEARCH. (ABINGDON, 21-23 JUNE 1983)

WCP - 61 REPORT OF THE EXPERT GROUP MEETING ON THE CLIMATIC SITUATION AND DROUGHT IN AFRICA (GENEVA, 6 - 7 OCTOBER, 1983) (also available in French)

WCP - 62 REPORT OF THE FIRST SESSION OF THE JSC/CCCO TOGA SCIENTIFIC STEERING GROUP (HAMBURG, 25-27 AUGUST 1983)

WCP - 63 THE NUMERICAL CLASSIFICATION OF THE WORLD'S CLIMATES. By Joseph K. Litynski (also available in French)

WCP - 64 REPORT OF THE MEETING ON CLIMATE SYSTEM MONITORING. (GENEVA, 5-9 DECEMBER 1983)

WCP - 65 REPORT OF THE FIRST CO-ORDINATION MEETING ON SOUTHERN AFRICAN DEVELOPMENT CO-ORDINATION CONFERENCE (SADCC) CLIMATE DATA MANAGEMENT AND USER SERVICES. (HARARE, 21-25 NOVEMBER 1983)

WCP - 66 REPORT OF THE FIRST SESSION OF THE CCl WORKING GROUP ON DATA MANAGEMENT (WGDM). (GENEVA, 7-11 NOVEMBER 1983)

WCP - 67 CLIMATE APPLICATIONS REFERRAL SYSTEM - CARS FOOD. (GENEVA, DECEMBER 1983)

WCP - 68 REPORT OF THE WORKSHOP ON INTERIM OCEAN SURFACE WIND DATA SETS. (MADISON, WISCONSIN, USA, 25-27 OCTOBER 1983) (out of print)

WCP - 69 REPORT OF THE FIRST SESSION OF THE JSC/CCCO WOCE SCIENTIFIC STEERING GROUP (WOODS HOLE, USA, 3-5 AUGUST 1983)

WCP - 70 REPORT OF AN INTERNATIONAL MEETING OF EXPERTS ON SATELLITE SYSTEMS TO MEASURE THE EARTH'S RADIATION BUDGET PARAMETERS AND CLIMATE CHANGE SIGNALS (IGLS, AUSTRIA, 29 AUGUST - 2 SEPTEMBER 1983)

WCP - 71 REPORT OF THE FIFTH SESSION OF THE JSC WORKING GROUP ON NUMERICAL EXPERIMENTATION (CHATEAU DU RY, FRANCE, 1-4 NOVEMBER 1983)

WCP - 72 REPORT OF THE PROBLEM OF CLIMATE AND CLIMATE VARIATIONS BY J. SMAGORINSKY - DECEMBER 1983

WCP - 73 THE INTERNATIONAL SATELLITE CLOUD CLIMATOLOGY PROJECT (ISCCP) - CLOUD ANALYSIS ALGORITHM INTERCOMPARISON. March 1984

WCP - 74 REPORT OF THE WMO EXPERT MEETING ON ATMOSPHERIC BOUNDARY LAYER PARAMETERIZATION OVER THE OCEANS FOR LONG-RANGE FORECASTING AND CLIMATE MODELS (READING, U.K., 5-9 DECEMBER 1983)

WCP - 75 RAINFALL PATTERNS IN THE DESERT. By Louis Berkofsky

WCP - 76 REPORT OF THE MEETING OF EXPERTS ON THE DESIGN OF A PILOT ATMOSPHERIC HYDROLOGICAL EXPERIMENT FOR THE WCRP (GENEVA, 28 NOVEMBER-2 DECEMBER 1983)

WCP - 77 REPORT OF THE MEETING OF EXPERTS ON SEA-ICE AND CLIMATE MODELLING (GENEVA, 12-16 DECEMBER 1983)

WCP - 78 REPORT OF THE MEETING OF EXPERTS ON CLIMATE AND HUMAN HEALTH (GENEVA, 5-9 DECEMBER 1983)

WCP - 79 CLIMATE APPLICATIONS REFERRAL SYSTEM (GENEVA, APRIL, 1984)

WCP - 80 RAPPORT SUR L'EVALUATION DE LA RESSOURCE ENERGETIQUE SOLAIRE A L'AIDE DE SATELLITES METEOROLOGIQUES par N. Beriot

WCP - 81 REPORT OF THE SECOND SESSION OF THE JSC/CCCO WOCE SCIENTIFIC STEERING GROUP (WORMLEY, UK, 23-28 JANUARY 1984)

WCP - 82 REPORT OF THE THIRD SESSION OF THE INTERNATIONAL WORKING GROUP ON DATA MANAGEMENT FOR THE INTERNATIONAL SATELLITE CLOUD CLIMATOLOGY PROJECT (ISCCP). (TOKYO, 6-8 MARCH 1984)

WCP - 83 REPORT OF THE STUDY CONFERENCE ON SENSITIVITY OF ECOSYSTEMS AND SOCIETY TO CLIMATE CHANGE. (VILLACH, AUSTRIA, 19-23 SEPTEMBER 1983)

WCP - 84 BIBLIOGRAPHY OF CLIMATE TEXTBOOKS AND STUDIES. By Malcolm Rigby

WCP - 85 QUALITY CONTROL OF CLIMATOLOGICAL SURFACE DATA. By P.F. Abbott

WCP - 86 EXTRAPOLATION OF MEAN WIND STATISTICS WITH SPECIAL REGARD TO WIND ENERGY APPLICATIONS. By Niels Otto Jensen, Erik Lundtang Petersen and Ib Troen